geodiversitas

2022 • 44 • 10

Skeleton of Early Miocene *Bathyergoides neotertiarius* Stromer, 1923 (Rodentia, Mammalia) from Namibia: behavioural implications

Laura BENTO DA COSTA & Brigitte SENUT

art. 44 (10) — Published on 10 March 2022
www.geodiversitas.com

PUBLICATIONS SCIENTIFIQUES

MUSÉUM NAL HIST NATURELLE

Geodiversitas est indexé dans / Geodiversitas *is indexed in:*
– Science Citation Index Expanded (SciSearch®)
– ISI Alerting Services®
– Current Contents® / Physical, Chemical, and Earth Sciences®
– Scopus®

Geodiversitas est distribué en version électronique par / Geodiversitas *is distributed electronically by:*
– BioOne® (http://www.bioone.org)

Les articles ainsi que les nouveautés nomenclaturales publiés dans *Geodiversitas* sont référencés par / *Articles and nomenclatural novelties published in* Geodiversitas *are referenced by:*
– ZooBank® (http://zoobank.org)

Geodiversitas est une revue en flux continu publiée par les Publications scientifiques du Muséum, Paris
Geodiversitas *is a fast track journal published by the Museum Science Press, Paris*

Les Publications scientifiques du Muséum publient aussi / *The Museum Science Press also publish:* ***Adansonia***, ***Zoosystema***, ***Anthropozoologica***, ***European Journal of Taxonomy***, ***Naturae***, ***Cryptogamie*** **sous-sections** ***Algologie***, ***Bryologie***, ***Mycologie, Comptes Rendus Palevol***

Diffusion – Publications scientifiques Muséum national d'Histoire naturelle
CP 41 – 57 rue Cuvier F-75231 Paris cedex 05 (France)
Tél. : 33 (0)1 40 79 48 05 / Fax : 33 (0)1 40 79 38 40
diff.pub@mnhn.fr / http://sciencepress.mnhn.fr

ISSN (imprimé / *print*) : 1280-9659/ ISSN (électronique / *electronic*) : 1638-9395

Skeleton of Early Miocene *Bathyergoides neotertiarius* Stromer, 1923 (Rodentia, Mammalia) from Namibia: behavioural implication

Laura BENTO DA COSTA
Centre de Recherche en Paléontologie – Paris (Sorbonne Université – MNHN – CNRS),
Campus Pierre et Marie Curie T.46-56, E.5, case 104, 4 Place Jussieu, 75252 Paris cedex 05 (France)
and Institut des Sciences de la Terre de Paris (Sorbonne Université-CNRS), Sorbonne Université,
Campus Pierre et Marie Curie T.56-55, E.5, case 116, 4 Place Jussieu, 75252 Paris cedex 05 (France)
laura.bento_da_costa@sorbonne-universite.fr (corresponding author)

Brigitte SENUT
Centre de Recherche en Paléontologie – Paris (Sorbonne Université – MNHN – CNRS),
Muséum national d'Histoire naturelle, CR2P-UMR,
case postale 38, 43 rue Buffon, 75005, Paris (France)
brigitte.senut@mnhn.fr

Submitted on 2 February 2020 | accepted on 10 July 2020 | published on 10 March 2022

urn:lsid:zoobank.org:pub:97D9B1D3-CBAC-41E8-B913-44AC67FCAAA3

Bento Da Costa L. & Senut B. 2022. — Skeleton of Early Miocene *Bathyergoides neotertiarus* Stromer, 1923 (Rodentia, Mammalia) from Namibia: behavioural implications. *Geodiversitas* 44 (10): 291-322. https://doi.org/10.5252/geodiversitas2022v44a10. http://geodiversitas.com/44/10

ABSTRACT
Essentially known from dental remains, the species *Bathyergoides neotertiarius* Stromer, 1923 (Bathyergidae, Rodentia) is widely recorded in Lower Miocene sites, notably in the localities of Elisabethfeld, Grillental and Langental (Namib Desert, Namibia). On the basis of dental morphology, this species belongs to the Bathyergidae, an extant family represented by the mole rats, which developed a fossorial, predominantly subterranean lifestyle. The discovery of a skeleton in connexion at the locality of GT Carrière (Grillental) permits description for the first time of the postcranials of *Bathyergoides neotertiarius*. Comparisons with extant rodent species suggest a similar behaviour to the Miocene ones, showing burrowing adaptations using principally the skull/mandible/incisor complex, evidenced by an accentuated robustness of these structures. The results of the postcranial analysis confirm the previous hypothesis, showing a robust anterior limb, probably used for the extraction of material during digging. However, a difference is seen in the robustness of the hind limb, being gracile in GT 50'06, but showing a prominent *m. popliteus* process, which suggests an important stabilization of the knee joint and an internal rotation of the lower limb allowing postural control in the burrows. The presence of a long tail distinguishes the Lower Miocene species from the extant subterranean rodents which exhibit short tails and recalls the morphology seen in modern semi-fossorial scratch-diggers such as *Cricetomys gambianus* Waterhouse, 1840. Thus, the specimen GT 50'06 shows clear fossorial adaptations, with a morphology close to the chisel-tooth diggers but exhibiting characteristics useful for a scratch-digging strategy.

KEY WORDS
Rodentia,
Bathyergidae,
Namibia,
Grillental,
Lower Miocene,
dental morphology,
postcranial morphology,
fossorial adaptations.

RÉSUMÉ
Le squelette de Bathyergoides neotertiarius *Stromer, 1923 (Rodentia, Mammalia) du Miocène inférieur de Namibie : implications comportementales.*
Essentiellement connue par des restes dentaires, l'espèce *Bathyergoides neotertiarius* Stromer, 1923 (Bathyergidae, Rodentia) est largement représentée dans les sites du Miocène inférieur, notamment dans les localités d'Elisabethfeld, Grillental et Langental (Désert du Namib, Namibie). Sur la base de la morphologie dentaire, cette espèce appartient aux Bathyergidae, famille actuelle représentée par les rats taupes africains, qui ont développé un mode de vie fouisseur, essentiellement souterrain. La découverte d'un squelette en connexion dans la localité de GT Carrière (Grillental) permet pour la première fois de décrire le matériel postcrânien de *Bathyergoides neotertiarius*. Les comparaisons avec les rongeurs actuels suggèrent un comportement similaire chez les espèces miocènes, montrant des adaptations au fouissage utilisant principalement le complexe crâne/mandibule/incisives, mis en évidence par une robustesse accentuée de ces structures. Les résultats des analyses sur le postcrânien confirment cette hypothèse, montrant un membre antérieur robuste, probablement utilisé dans l'extraction de matériel durant le fouissage. Cependant, une différence est présente dans la robustesse du membre postérieur, gracile chez GT 50'06, mais possédant une saillie proéminente pour l'insertion du *m. popliteus*, suggérant une importante stabilisation du genou ainsi qu'une rotation interne du membre permettant le maintien de la posture dans les terriers. La présence d'une longue queue distingue l'espèce du Miocène inférieur des rongeurs souterrains actuels qui ont des queues courtes, mais la rapproche des rongeurs semi-fouisseurs *scratch-diggers* (fouisseurs avec les membres antérieurs) tels que *Cricetomys gambianus* Waterhouse, 1840. Ainsi, le spécimen GT 50'06 montre des adaptations claires au fouissage, avec une morphologie proche des *chisel-tooth diggers*, mais montrant cependant des caractéristiques utiles pour l'utilisation de la stratégie de *scratch-digging*.

MOTS CLÉS
Rodentia,
Bathyergidae,
Namibie,
Grillental,
Miocène inférieur,
morphologie dentaire,
morphologie
postcrânienne,
fouissage.

INTRODUCTION

Well known in Subsaharan Africa, Bathyergids are today represented by the African mole rats. They are found in different kinds of habitats, from open forested environments to savannas and arid semi-desert/desert landscapes (Happold *et al.* 2013). Bathyergids are exclusively fossorial, a behaviour reflected in the morphology of the skull and mandible which are robust and bear large incisors for burrowing activities (Stuart & Stuart 2015). Since 1992, surveys of the Namibia Palaeontology Expedition in the Lower Miocene of the Sperrgebiet (Forbidden Area due to diamond mining activities) have yielded a rich microfauna, including remains of several rodent families (Diamantomyidae, Thryonomyidae, Sciuridae, Cricetidae, Pedetidae and Bathyergidae) (Stromer 1926; Pickford & Senut 2000). The fossils described herein were found at Grillental, Elisabethfeld, Fiskus and Langental (aged between 20 and 19 million years) which are located in the Northern Sperrgebiet (South of Lüderitz, Namibia) (Pickford & Senut 2000). Most of the bathyergid specimens are represented by craniodental and mandibular remains, belonging to the species *Bathyergoides neotertiarius* Stromer, 1923 erected by Stromer in 1923 on the basis of two fragments of mandibles and an m2 (belonging to the right mandibular fragment) discovered at Langental. The main characteristics of *Bathyergoides neotertiarius* are: a high skull, large infraorbital foramen, five lower cheek teeth with three principal crests, four upper ones with four crests, the robust incisors extending beyond the M3 (Stromer1923; Lavocat1973). More recently, new craniodental and mandibular specimens were studied by Mein & Pickford (2008). However, no postcranial remains were described. This is why the discovery at Grillental in 2006 of a partial skeleton in connection, gives the opportunity to fill this gap and the possibility to apprehend the behaviour of the fossil species.

GEOLOGY

Dated at 20 to 19 million years (Lower Miocene) by biochronology, Grillental is located in the North of the Sperrgebiet Area 1 within the Namib Desert (Namibia) (Fig. 1). This site was formed in a flood-plain context, within the Proto-Kaukausib drainage in which fluvial sediments accumulated (Pickford & Senut 2000). The Oligocene palaeovalley was filled by Miocene sediments consisting of green clays overlying the basement and which are overlain by coarse-grained fluvial sands. A large deposit of travertine and aeolianites unconformably overlying the fossiliferous clays is observed in the West of Grillental (Pickford 2008).

At Grillental, several localities have been identified among which, GT Carrière yielded the specimen studied herein (Figs 2; 3).

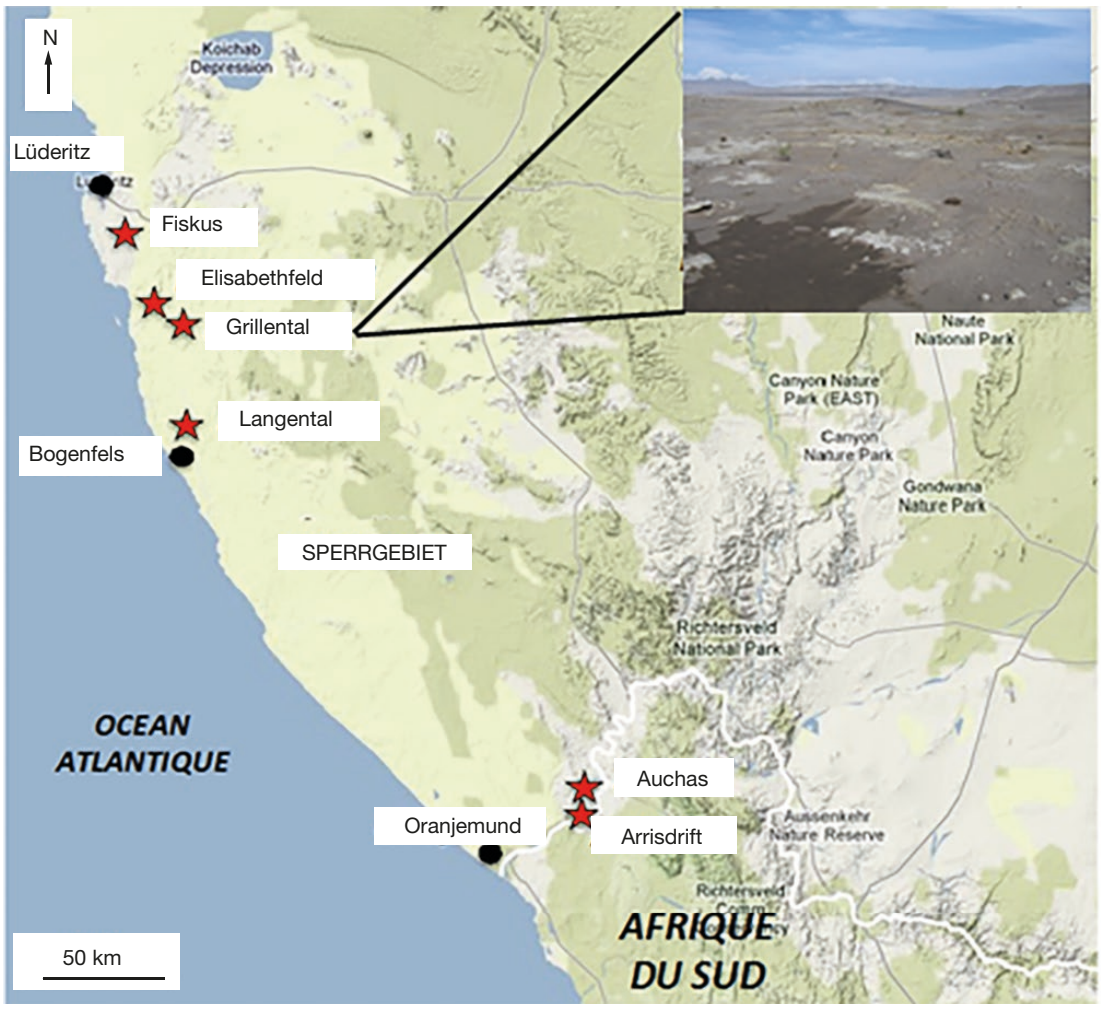

Fig. 1. — Map of the Sperrgebiet (Diamond Area 1, Namib Desert, Namibia) and location of the palaeontological sites (modified after Roche 2012).

Fig. 2. — GT Carrière, at the base of the dune, the green clay levels yielded the fossils.

Fig. 3. — Skeleton of *Bathyergoides neotertiarius* Stromer, 1923 (GT 50'06) in situ when discovered.

MATERIAL AND METHODS

Collected in January 2006, the partial skeleton in connection GT 50'06, preserves the skull, the two hemi-mandibles and some postcranial elements. Different nomenclatures have been used for the descriptions: for the teeth, Rodrigues & Šumbera, 2015, adapted from Mein & Pickford (2008) and for cranial and postcranial remains, Grassé & Gabe (1967) and Kahle *et al.* (1992).

Measurements and pictures were taken with a Q-Scope Digital Microscope QS.90200-P calibrated in millimetres (mm), for the small dental and postcranial specimens. The skeletal fragments were measured with calipers, and images were taken with an Olympus Tough 4 camera (Fig. 4). Two morphological indices have been used for the humeral comparisons between the fossil and extant specimens: the epicondyle index and the humeral robusticity index, established by Price (1993). The epicondyle index is the ratio between the width of the distal epiphysis and the total length of the humerus. It indicates the available surface for the insertion of the flexor, pronator and supinator muscles of the fore-arm involved in fossorial activities. The humeral robusticity index shows the ability of the humeral shaft to resist bending and shearing stresses. This index represents the ratio between the width of the shaft and the total length of the humerus (Price 1993; Lagaria & Youlatos 2006) (Fig. 4).

The extant rodent specimens used for this study are curated in different Museum collections: The Museum national d'Histoire Naturelle (Paris, France), The Ditsong Museum (Pretoria, South Africa) and the Royal Museum of Central Africa (Tervuren, Belgium).

ABBREVIATIONS

Concerning the dental descriptions, abbreviations for the upper cheek teeth are Px and Mx, while the lower cheek teeth are designated px and mx. The dental formula is specified in the description.

SYSTEMATIC PALAEONTOLOGY

Order RODENTIA Bowdich, 1821
Suborder HYSTRICOMORPHA Brandt, 1855
Infraorder HYSTRICOGNATHI Brandt, 1855
Family Bathyergidae Waterhouse, 1841
Subfamily Bathyergidae Waterhouse, 1841

Genus *Bathyergoides* Stromer, 1923

Type species. — *Bathyergoides neotertiarius* Stromer, 1923

Bathyergoides neotertiarius Stromer, 1923

Emended diagnosis by Lavocat 1973. — The complete series of the lower cheek teeth consists of five (sic) teeth; there are four upper cheek teeth bearing four crests, the paracone crest usually separated from the protocone, sometimes fused with wear; crest of the metacone always separated. Skull very high, with a very characteristic wedge shape. Posterior area of the skull anteroposteriorly very short. Large infraorbital foramen. Strong upper incisor which reaches the top of the root of the M3. Lower incisor touching the anterior face of the condyle, anteriorly to this one.

Holotype. — A fragment of right mandible with the m2 and an isolated lower molar.

Material examined. — GT 50'06 (Skull and mandible with P4-M3/p4-m3, incisors, partial skeleton), LT 200b'98 (right mandible with p4-m3), LT 50'19 (right mandible with p4-m3).

Dental formula. — 1.0.1.3/1.0.1.3

DESCRIPTION OF SKULL, MANDIBLE AND TEETH

Incisors (Fig. 5)
The left upper incisor was found isolated, while the lower ones are preserved in the mandibles (Fig. 4). The incisors are robust, triangular in transverse section. A thick layer of brown enamel is present on the external surface of the teeth, not extending beyond the first third of the labial surface. The radicular end of the lower incisors

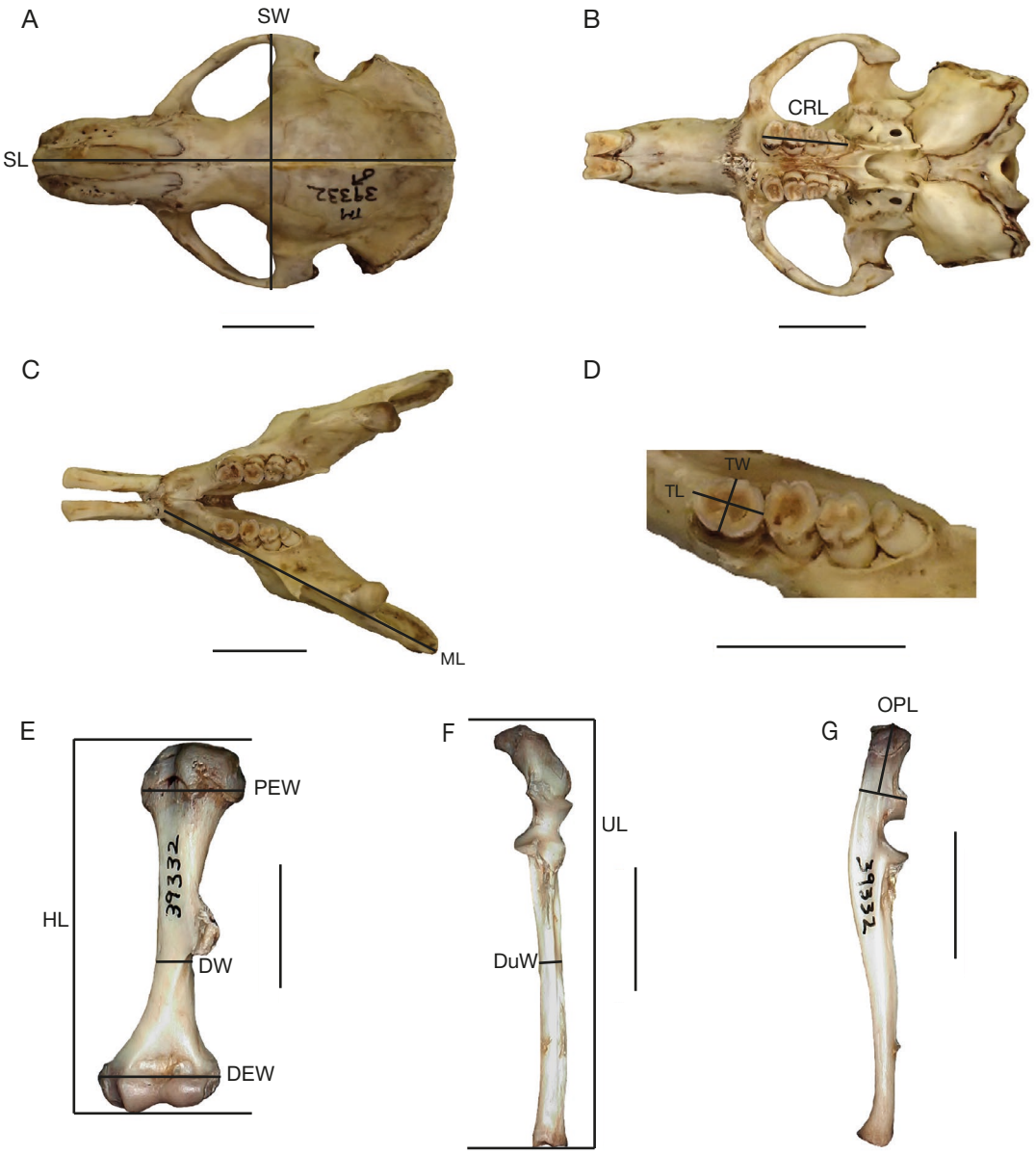

Fig. 4 — List of measurements taken in this study and used for the index calculations. *Bathyergus janetta* Thomas and Schwann, 1904, specimen TM 39332 : **A**, dorsal view of the skull; **B**, ventral view of the skull; **C**, dorsal view of the mandible; **D**, occlusal view of the left cheek teeth raw; **E**, anterior view of the left humerus; **F**, anterior view of the left ulna; **G**, medial view of the left ulna. Abbreviations: **SL**, length of the skull; **SW**, width of the skull; **CRL**, length of the cheek teeth raw; **ML**, length of the hemimandible; **HL**, length of the humerus; **DW**, length of the humeral diaphysis; **DEW**, width of the distal epiphysis; **PEW**, width of the proximal epiphysis; **UL**, length of the ulna; **DuW**, width of the ulna diaphysis; **OPL**, length of the olecranon process; **TL**, length of the tooth; **TW**, width of the tooth. Scale bars: 1 cm.

terminates close to the base of the articular condyle, well beyond the m3.

The premolars and molars exhibit the same structures. The p4 and P4 are smaller than the molars. The m2 and M2 are the biggest cheek teeth; the m3 and M3 are always smaller than the m2 and M2.

P4-M1-M2-M3 (Table 1; Fig. 6)

The upper premolars and molars are wider than long. The teeth are lightly worn, showing the outer groove and forming a crescent-shaped fossa, which disappears with advanced wear. The protocone and hypocone are connected to a small endoloph. The lingual sinus is poorly developed, slit-shaped when the tooth is slightly worn. The anteroloph extends from the protocone and joins the anterior face of the paracone. This crest, fused with the paracone, forms the anterior border of the tooth. The paracone and metacone are centred on the buccal margin of the tooth. Depending on the wear, these cusps tend to fuse, the metacone being more prominent than the paracone. It should be noted that there is a problem concerning the definition of the metacone which will be treated in the discussion.

The posterior part of the cheek teeth looks like the anterior part, the posteroloph forming the posterior wall of the teeth. It extends from the posterior face of the hypocone to

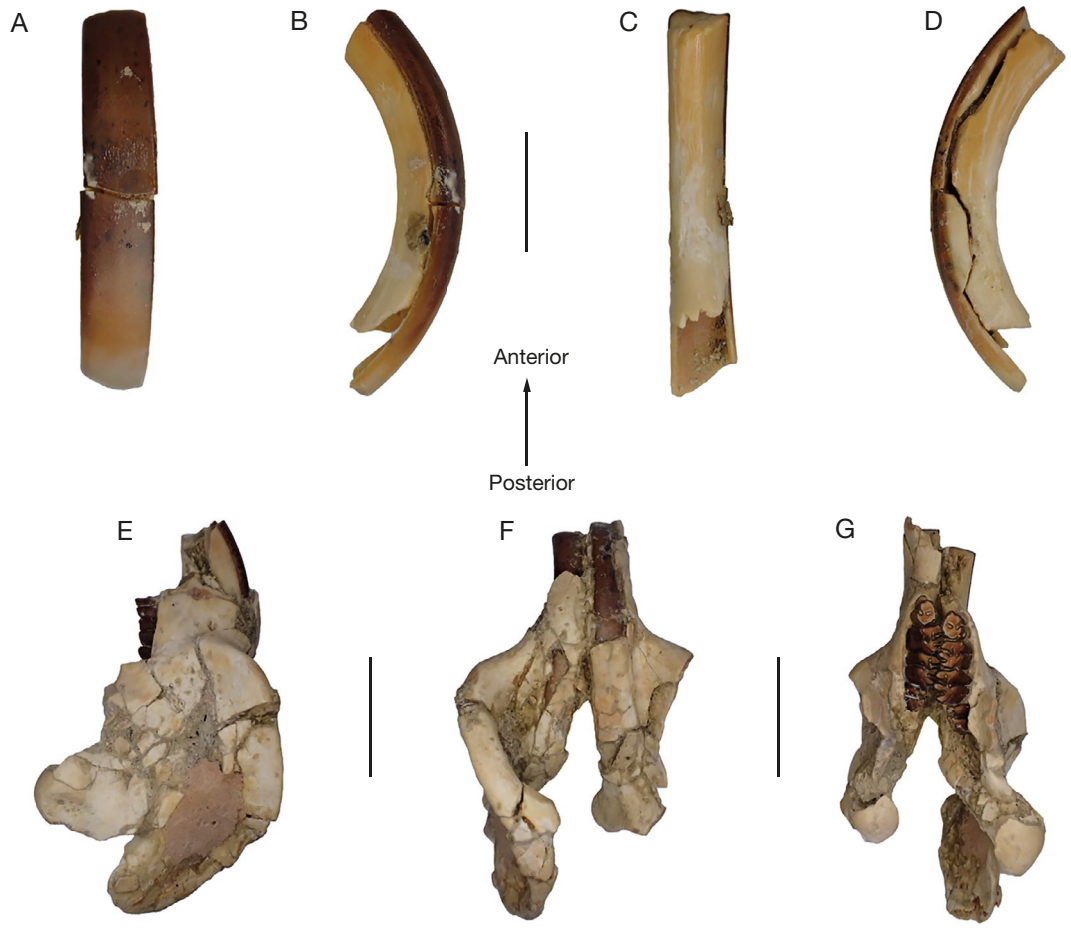

Fig. 5 — Upper Incisor and mandible of GT 50'06: **A-D**, left upper incisor; **A**, labial view; **B**, mesial view; **C**, lingual view; **D**, distal view. E-G, mandible; **E**, right lateral view; **F**, inferior view; **G**, occlusal view. Scale bars: 1 cm.

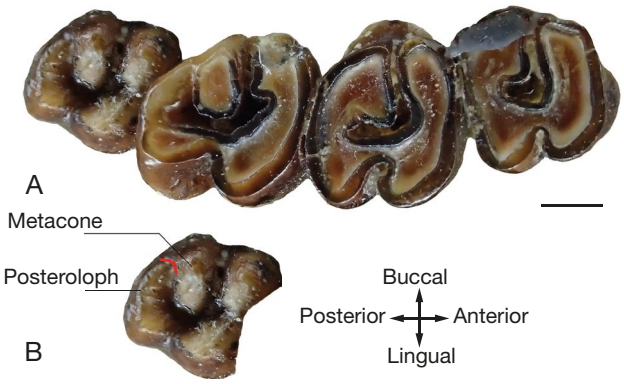

Fig. 6. — Right upper cheek tooth row of GT 50'06: A, P4-M3, B, detail of the posterior part of the M3 (occlusal view) with the separation between the posteroloph and the metacone (in red). Scale bar: 1 mm.

Fig. 7. — Right lower cheek tooth row of GT 50'06 (p4-m3, occlusal view). Scale bar: 1 mm.

Table 1. — Measurements of the right upper and lower cheek teeth of the specimen GT 50'06.

Mesio-distal length				Bucco-lingual breadth			
P4	**M1**	**M2**	**M3**	**P4**	**M1**	**M2**	**M3**
3.004	3.288	3.831	>3.266	3.488	3.735	3.75	>3.403
p4	**m1**	**m2**	**m3**	**p4**	**m1**	**m2**	**m3**
3.349	3.532	4.184	>3.37	3.031	3.505	4.184	>3.128

the posterobuccal surface of the metacone. During wear, the posteroloph does not join the metacone in the M3; the latter cusp forming the posterobuccal border of the tooth.

p4-m1-m2-m3 (Table 1; Fig. 7)

Buccolingually, the p4 is narrower anteriorly than posteriorly. The metaconid projects anteriorly forming the mesial margin of the tooth. The structures are poorly identifiable due to advanced wear. The structure of the p4 is similar to that of the molars. The central furrow is reduced to an islet of enamel

Fig. 8. — Views of the skull GT 50'06 before cleaning. Scale bar: 1 cm.

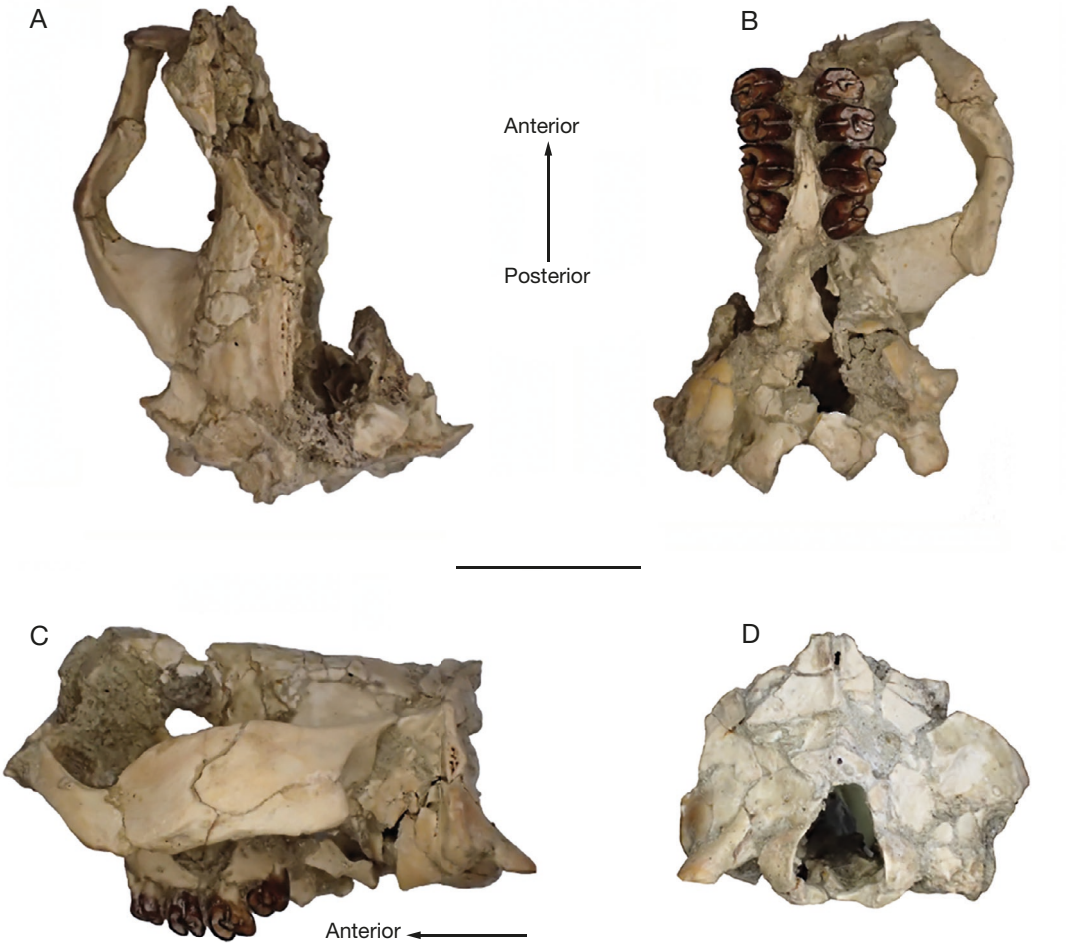

Fig. 9. — Skull of GT 50'06: **A**, dorsal view; **B**, ventral view; **C**, left lateral view; **D**, occipital view. Scale bar: 1 cm.

and the posterior one is reduced to a small notch on the posterolingual border. The lower molars present three principal crests (metalophulid I, entolophid and posterolophid). The posterior part of the tooth is slightly narrower buccolingually than the anterior one, the posterolophid being shorter than the other two crests. This shortening is more marked in the m3s which are still erupting and are therefore lightly worn.

The protoconid and the hypoconid are prominent and connected by a short ectolophid. The narrow buccal V-shaped sinusid is limited by these three structures. It is buccoanteriorly to posterolingually oriented. A short metalophulid I extends from the anterior face of the protoconid to the anterolingual side of the metaconid forming the anterior wall of the tooth. The hypoconid is

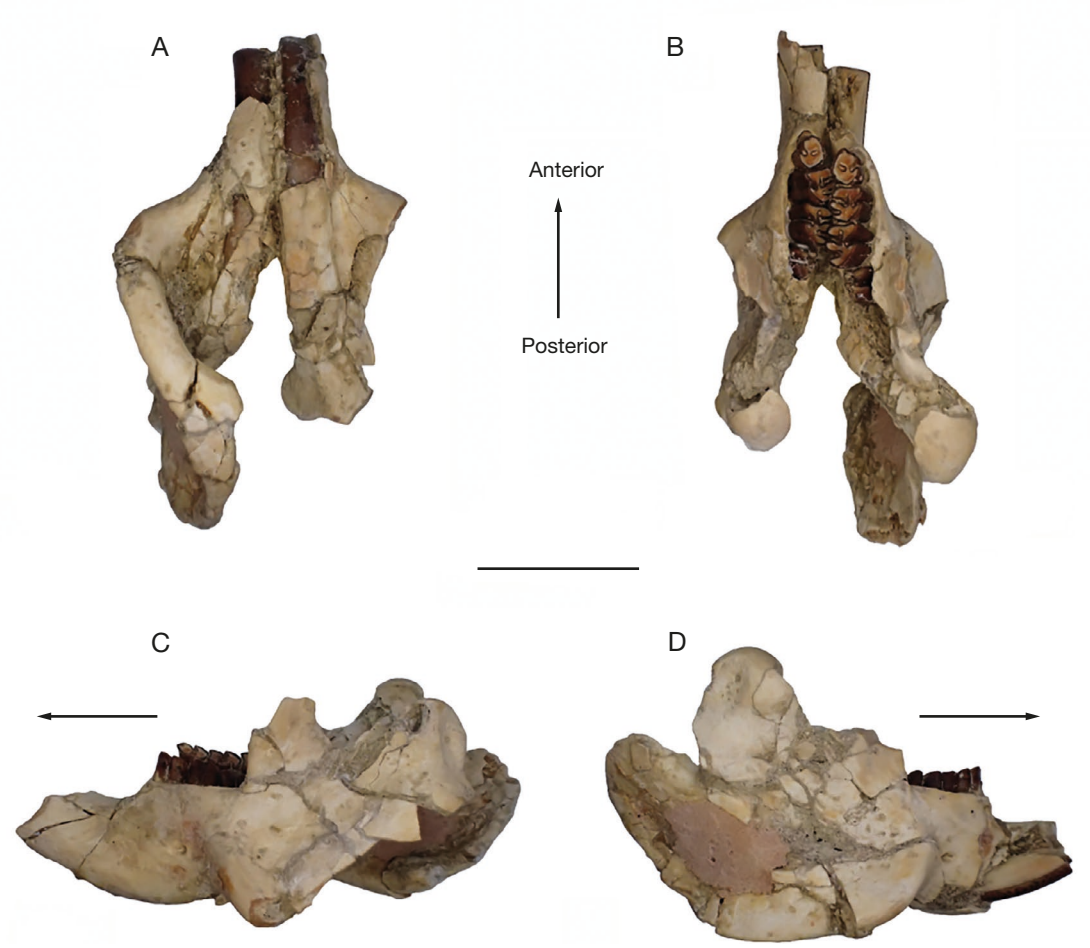

Fig. 10. — Mandible of GT 50'06: **A**, ventral view; **B**, dorsal view; **C**, left buccal view; **D**, right buccal view. Scale bar: 1 cm.

connected to the prominent entoconid by a short crest: the entolophid. Due to the advanced degree of wear, the hypoconid, entolophid and entoconid are fused together forming the central crest. The posterolophid stretches from the posterior face of the hypoconid to the lingual border of the tooth.

Skull (Figs 8; 9)
The fragmentary skull is slightly deformed due to compaction and to fossilization in salty and gypsiferous deposits. It preserves the palate with the tooth rows, the left zygomatic arch and a part of the occipital areas.

Dorsal view
The left zygomatic arch projects strongly laterally, resulting in a great width of the skull with a rounded aspect of the lateral side. It gradually enlarges backwards. Despite the poor preservation of the cranial roof, a marked sagittal crest can be seen.

Ventral view
The tympanic bullae are ovoid and not prominent. The left paracondylar process is preserved and shows a strong posterior development, which terminates at the level of the occipital condyle. The triangular mastoid process is well developed. The tooth rows are parallel (probably partially due to compaction), on both sides bordering a thin palatine bone. Close to the M2s, a round and deep foramen occurs in the middle of the palatine bone.

Lateral view
The left zygomatic arch is massive, thickened (tall) in its middle part. The maximum height is reached at the junction of the zygomatic bone and the temporal bone. The frontal process of the zygomatic bone extends above the end of the zygomatic process of the temporal bone. The inferior part of the anterior end of the zygomatic arch extends well below the zygomatic process of the temporal bone. The height of the arch decreases backwards towards the temporal bone. Despite the compaction, it is possible to estimate the proportions of the skull: the posterior part of the skull being shorter than the palatal one (1.74 cm against 1.2 cm).

Occipital view
In occipital view, the skull is wider than tall. The preservation of the occipital surface does not permit precise description of the basioccipital, the exoccipital and the supraoccipital bones. However, we observe that the occipital bones join at the level of the supraoccipital to form a prominent sagittal crest. The foramen magnum is ovoid, facing backwards, flanked at its base by the two rounded occipital condyles.

Fig. 11. — Lingual view of **A**, LT 200b'98; **B**, LT 50'19, specimens of *Bathyergoides neotertiarius*. Scale bar: 1 cm.

Mandible (Fig. 10)
The right hemi-mandible is well-preserved, except for the coronoid process, which is broken at its base, and the ascending ramus which is missing a slight fragment at its apex. The less well-preserved left hemi-mandible is missing the gonial area, the ascending ramus and the upper part of the coronoid process.

Buccal view
The hemi-mandibles are robust. In the right one, the masseteric fossa is large and deep. Despite the fact that the coronoid process is not entirely preserved, the remaining part suggests that it was higher than the articular condyle on the left mandible, agreeing with the morphology observed on other specimens of the species. The articular condyle is low. The mental foramen is deep and ovoid, located below the anterior part of the m1. The enamel extends onto the base of the lateral surface of the incisor.

Dorsal view
The horizontal ramus projects strongly laterally, at the level of the front of the m2, before curving gently backwards. Broken in its anterior part, the articular condyle is triangular in shape, transversely compressed and anterobucally/posterolingually elongated. The radicular end of the incisor extends beyond the back of the m3. The cheek tooth row is oriented in the plane of the incisor. The premolars and molars are in the same plane as in LT 50'19 and LT 200b'98 (Figs 10; 11), which show a slight difference in the orientation of the m2 and m3, certainly due to the stage of wear.

It is not possible to describe the lingual view of the mandible due to the state of preservation of the bones.

DESCRIPTION OF POSTCRANIAL ELEMENTS

Humerus (Fig. 12)
The right humerus and the proximal end of the left one are preserved. The bone is short and rather massive.

Anterior view
The *tuberculum majus* and *tuberculum minus* are poorly developed, the former extending proximally up to the top of the *caput humeri*. The *tuberculum minor* is lower than the *tuberculum major*. The posterior border of the *tuberculum major* joins distally the deltoid crest, which is strongly developed and extends as far as the two lower thirds of the bone. The *crista tuberculi minoris* is marked, descending distally as far as the middle of the humeral shaft. The *teres minor* tuberosity is weakly salient. The *sulcus intertubercularis* is shallow and broad. On the distal epiphysis, the *epicondylus medialis* is developed, with an inclination of 135° to the shaft axis. The *trochlea humeri* is mediolaterally short, bordered by a medial lip and slightly orientated downward. The distal part of the medial lip of the trochlea and the distal part of the capitulum are roughly at the same level. The capitulum is ovoid. The *epicondylus lateralis* is poorly developed and located above the capitulum. From the *epicondylus lateralis* extends the susepicondylar crest, forming a convex lateral border at its base, in contrast to the concave medial border of the humerus.

The *fossa radialis* is deep, large and perforated, connecting to the olecranon fossa. The *fossa coronoidea* is poorly marked. There is no sus-epitrochlear foramen.

Posterior view
The *caput humeri* is rounded and proximomedially to distolaterally oblique. The posterior humeral shaft is reinforced by a crest which provides insertion for the *m. triceps brachii*. The olecranon fossa is ovoid and wide and bordered by the medial and lateral pillars; the medial one being the wider.

Distally, the lateral and medial lips of the trochlea are parallel, inclined along the distomedial/proximolateral axis. The fossa olecrani is broad, perforated and delimited by two blunt, low crests.

Medial view
The *caput humeri* does not strongly project posteriorly above the humeral shaft. The deltoid crest is salient and flat on the anteromedial surface.

Lateral view
The posterior part of the diaphysis is flat but its anterior part is salient at midshaft level due to the development of the deltoid crest.

Proximal view:
The *caput humeri* is globular. The *tuberculum majus* is more salient anterolaterally than the *tuberculum minus* anteromedially. The *sulcus intertubercularis* is wide and shallow.

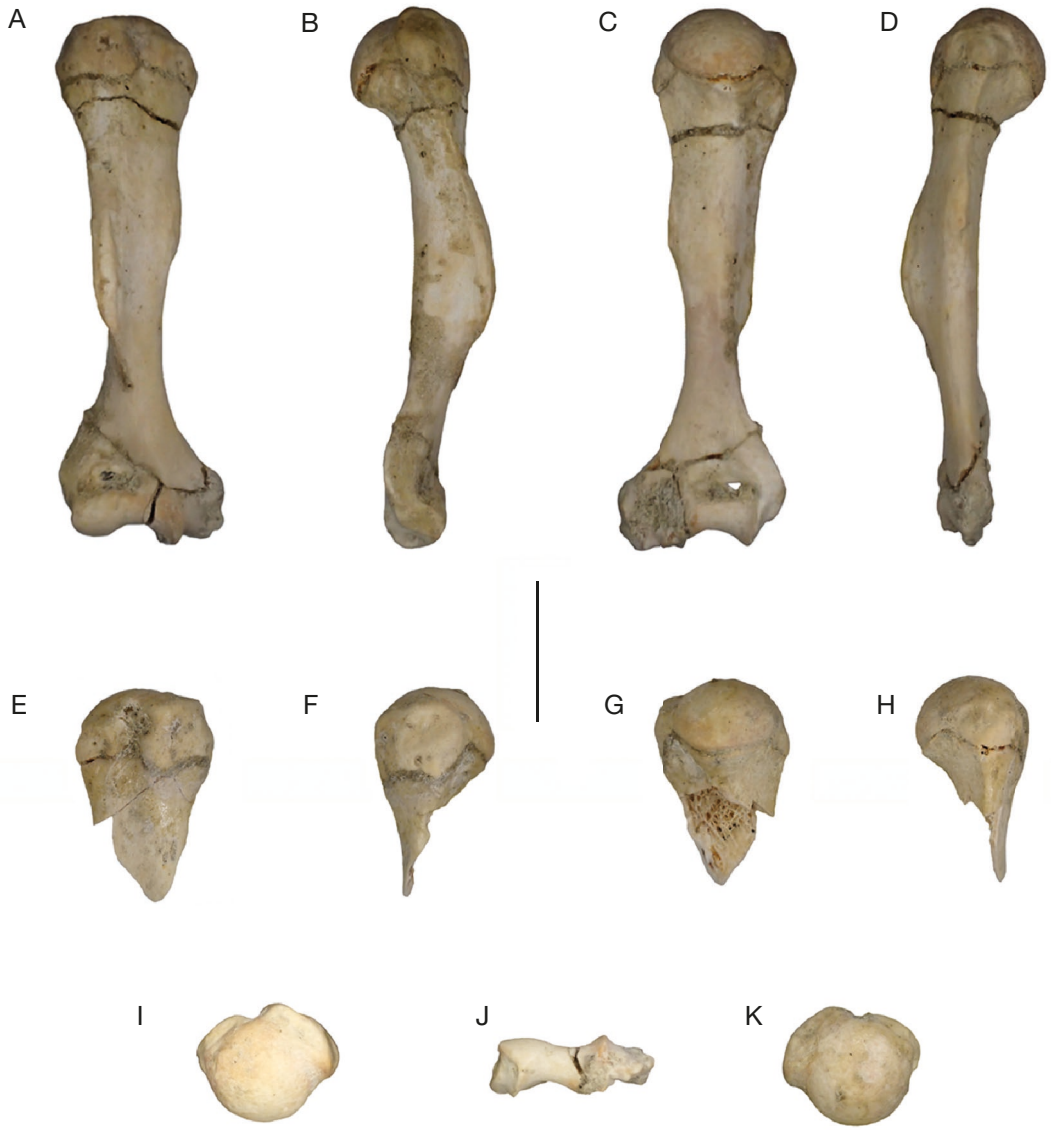

Fig. 12. — Humeri of GT 50'06: A-D, Right humerus; **A**, anterior view; **B**, lateral view; **C**, posterior view; **D**, medial view. E-H, Left humerus; **E**, anterior view; **F**, lateral view; **G**, posterior view; **H**, medial view. **I-J**, Proximal (**I**) and distal (**J**) view of the right humerus. **K**, proximal view of the left humerus. Scale bar: 1 cm.

Distal view
The capitulum is mediolaterally elongated, its anterior part being slightly higher than the medial lip of the trochlea. The lateral lip of the trochlea is posteriorly prominent. The *epicondylus medialis* is mediolaterally oriented, slightly oblique posteriorly. The *epicondylus lateralis* is poorly expressed.

Ulna (Fig. 13)
The right ulna is almost complete (>3.88 cm), missing only the styloid process and the most proximal part of the olecranon. The shaft is rather massive (only the width can be securely measured (0. 28 cm)). The left ulna preserves only the olecranon and the anconeal process.

Anterior view
The olecranon process is elongated, broadened in its proximal part. The *incisura trochlearis* is proximodistally elongated and proximolaterally to distomedially oblique. Its proximal part is wider than the distal part. The *incisura radialis* faces anterolaterally, and is not laterally salient. The ulnar tuberosity is elongated, with a central depression for the insertion of the *m. brachialis.* The shaft is straight and thickens distally. The *crista supinatora* is well marked and extends from the base of the *incisura radialis* to the distal end of the bone.

Lateral view
The bone exhibits a sigmoid curvature. The elongated olecranon (length = 0.7 mm) is bent forward. The anconeal and coronoid processes which limit the greater sigmoid cavity project equally anteriorly. The greater sigmoid cavity is semicircular. The *incisura radialis* is triangular with the apex pointing distally. A long and wide gutter is present on the lateral part, extending from the proximal part of the *incisura trochelaris* to the middle of the shaft.

Fig. 13. — Ulnae of GT 50'06: A-D, Right ulna; **A**, anterior view; **B**, lateral view; **C**, posterior view; **D**, medial view. E-F, Olecranon process of the left ulna; **E**, anterior view; **F**, lateral view; **G**, posterior view; **H**, medial view. Scale bar: 1 cm.

Medial view
The medial fossa of the olecranon is deep and large, extending to the level of the ulnar tuberosity. The anconeal fossa is deep and extends as far as the middle part of the ulnae.

Posterior view
The proximal end of the *incisura trochlearis* is strongly laterally salient, whereas the lower medial one is weakly medially developed.

Radius (Fig. 14)
The left radius only preserves its distal two thirds and the right is trapped within sediment. It is not possible to extract the right radius because of its fragility, but we can observe that it is almost complete despite the break. The right proximal epiphysis is preserved, flattened antero-posteriorly with a long neck and an elongated *tuberositas radii*. The *caput radii* is ovoid.

The radial shaft, which is more flattened in its proximal part, is rather thin and clearly widens at the distal epiphysis level, suggesting a reinforcement of the carpal area. On the ulnar side, two long crests run down and are separated by a long well-marked groove which broadens distally. These crests would give insertion to the *abductor pollicis longus* and *m. digitorum profundus*. The distal epiphysis of the radius is robust, the poorly salient *processus styloideus* being lower than the *facies articularis carpea*, which is not deep. Because of the poor preservation, it is not possible to confirm the existence of two articular surfaces for the lunate and the scaphoid. Despite its poor preservation the epiphysis appears triangular. A few carpal bones are preserved in the matrix, but are displaced and are not easily cleanable because of their fragility and will be part of another paper dealing with the hand of the species.

Femur (Fig. 15)
Despite the crushing, the proximal end and a fragment of diaphysis of the left femoral shaft, and a fragment of the right femoral shaft are preserved. The bone is massive and compressed anteroposteriorly. The left femoral condyles are fragmentary. The description is based on the left femur which is the better preserved.

Anterior view
The *tuberculus majus* (greater trochanter) is broken proximally, but the preserved part suggests that it is lower than the proximal part of the femoral head. The femoral neck is short and the proximal notch shallow. The third trochanter is elongated and weakly salient.

Posterior view
The *fossa trochanterica* (trochanteric fossa) is deep and broad. The femoral head is rounded. The neck is short and wide. The prominent *crista intertrochanterica* (posterior intertrochanteric crest) is well developed. The *tuberculus minus* (lesser trochanter) is broken proximally, and posteromedially oriented. The intertrochanteric crest forms an obtuse angle before joining the *tuberculus minus* (lesser trochanter).

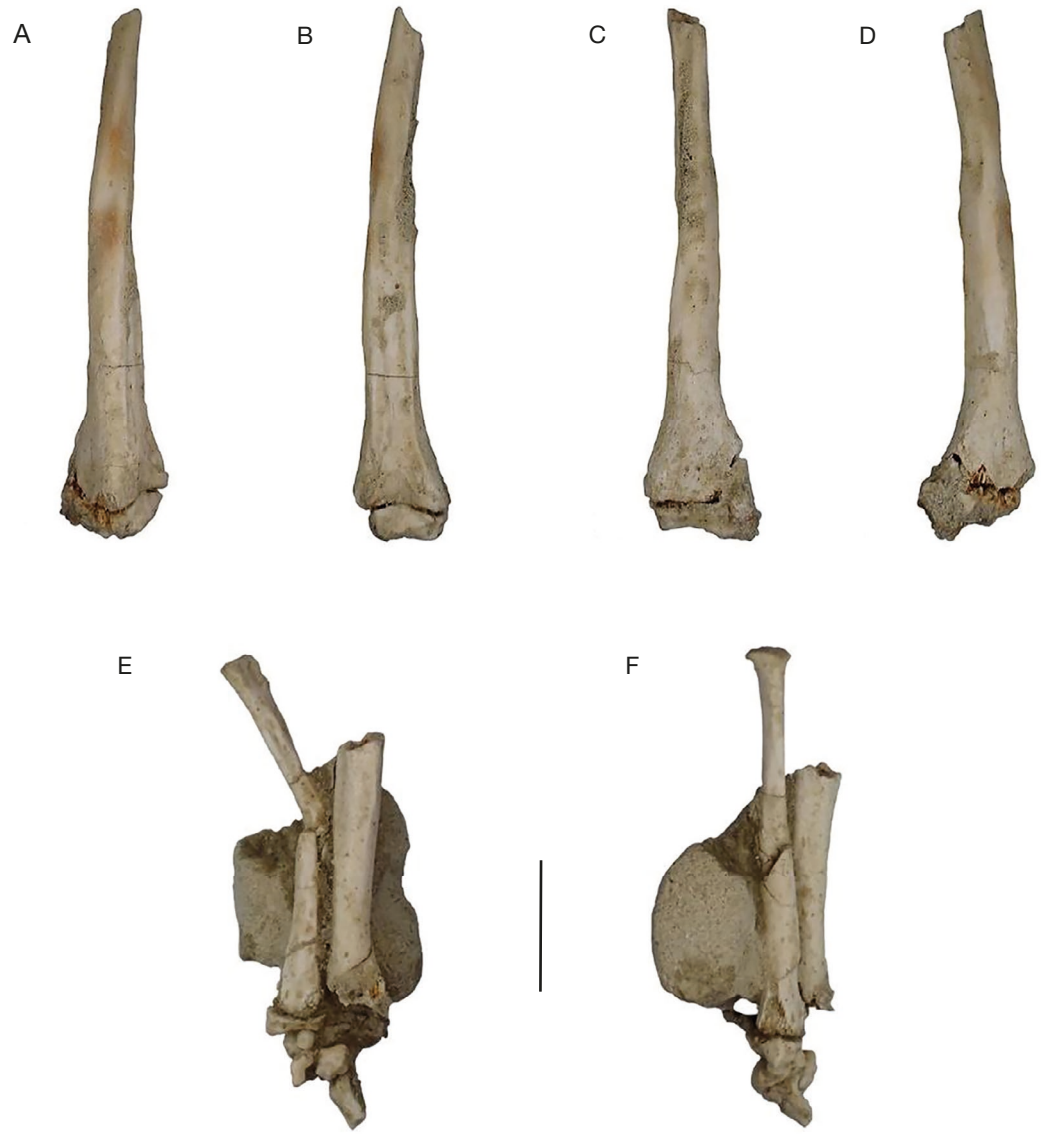

Fig. 14. — Radius of GT 50'06: A-D, Left radius: **A**, lateral view; **B**, medial view; **C**, anterior view; **D**, posterior view. E-F, Right radius and a fragment of the right ulna. **E**, medial view; **F**, anterior view. Scale bar: 1 cm.

Medial view
The neck and femoral head project anteriorly. The *fovea capitis* cannot be seen due to the poor preservation of the specimen.

Lateral view
The *tuberculus majus* (greater trochanter) projects slightly anteriorly. The third trochanter is represented by a slightly developed crest-shaped tuberosity. Its anterior surface is concave, while its posterior one is slightly convex.

Tibia and fibula (Figs 16; 17)
The proximal ends of the right tibia and fibula are preserved. The left tibia is almost complete, only the tibial plateau is missing. The left fibular shaft is preserved.

Anterior view
The tibia is lateromedially compressed, with an acerate tibial crest. The proximal end is laterally curved and the anterior tuberosity rectangular.

Posterior view
The fibula is fused with the fragmentary lateral condyle in the right specimen, and does not permit detailed description due to its poor preservation. There is no intercondylar eminence but it could be due to the state of the specimen. Posteromedially There is an elongated tuberosity at the side, where the *m. popliteus* inserts, which is salient distally. A slightly concave surface is present above the process, being the insertion of the *m. soleus*. These structures are separated from an elongated posteromedial gutter by a marked crest, which extends for one

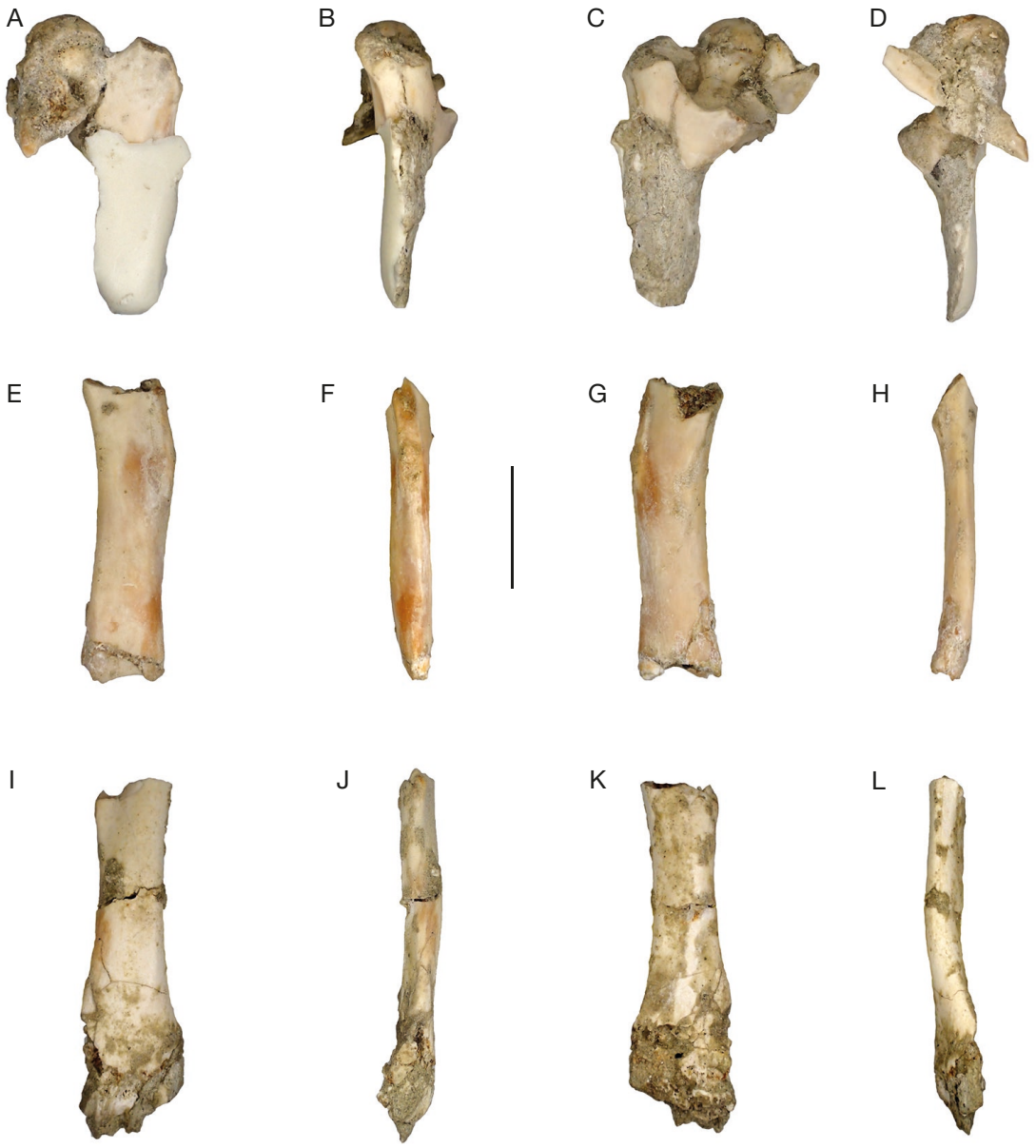

Fig. 15. — Femora of GT 50'06: A-D, Proximal epiphysis of the left femur; **A**, anterior view; **B**, lateral view; **C**, posterior view; **D**, medial view. E-H, Shaft of the right femur; **E**, anterior view; **F**, lateral view; **G**, posterior view; **H**, medial view. I-L, Shaft of the left femur; **I**, anterior view; **J**, lateral view; **K**, posterior view; **L**, medial view. Scale bar: 1 cm.

third of the bone. In this deep posteromedial gutter inserts the *m. tibialis posterior*.

Medial view
The medial surface is flat. The *m. popliteus* tuberosity is wide and convex, distally salient and posteromedially oriented. Above this protrusion, its posteromedial surface is slightly concave, where the *m. soleus* inserts.

Lateral view
The anterior tuberosity is convex. The tibial fossa for the insertion of a strong *m. tibialis anterior* is deep and broad. The crest separating the fossae of the *m. tibialis anterior* and the *m. tibialis posterior* is directed slightly backwards in its proximal part and extends downwards, disappearing progressively on the shaft.

Proximal view
The triangular tibial plateau is lateromedially compressed. The lateral condyle is developed and strongly posterolaterally projecting. Due to the poor preservation, it is not possible to describe precisely the groove, which does not seem to be deep. Because of the thinness of the tibia, unusual among rodents, it was difficult to determine the different muscular insertions; this is why we add an explicative figure (Fig. 17).

The left fibula shows a marked and elongated gutter on its anterior side. Despite the lack of its most proximal part, we observe that it is flared, corresponding to the junction with the tibial plateau.

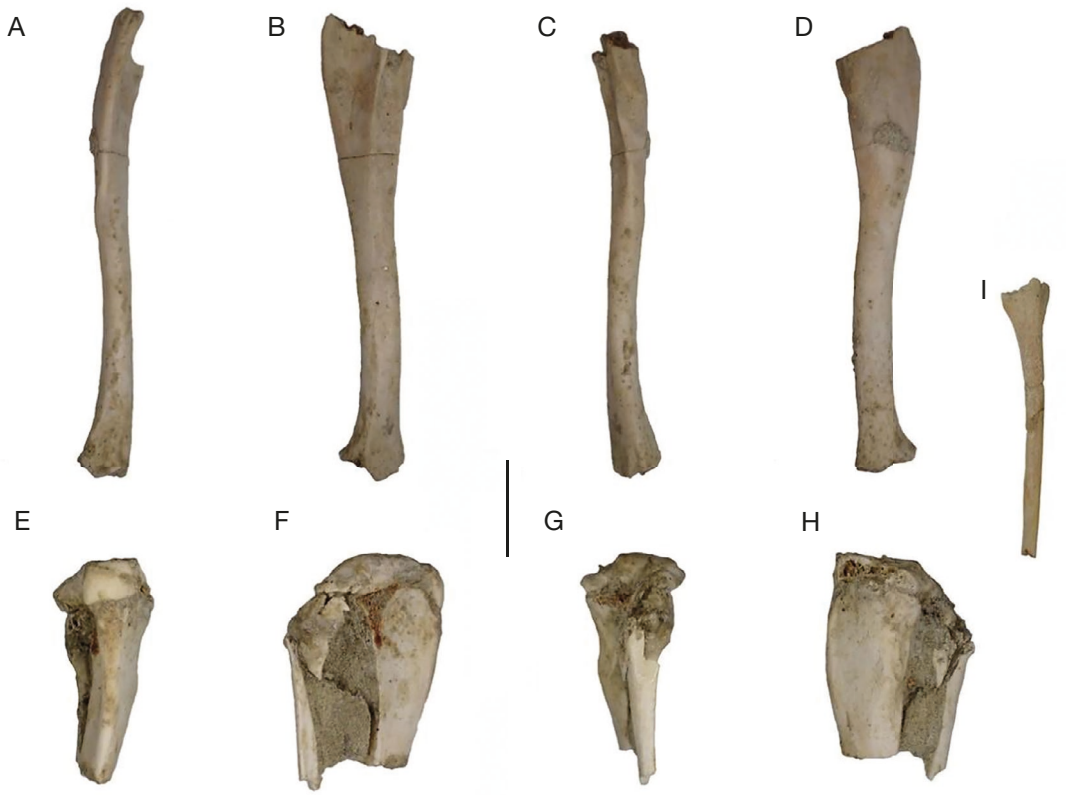

Fig. 16. — Tibiae of GT 50'06: **A**-**D**, Left tibia (**A**, anterior view; **B**, lateral view; **C**, posterior view; **D**, medial view); **E**-**H**, proximal epiphysis of the right tibia (**E**, anterior view; **F**, lateral view; **G**, posterior view; **H**, medial view;) I, left fibula. Scale bar: 1 cm.

Calcaneum (Fig. 18)

Only the left calcaneum is preserved, in connection with part of the astragalus which covers the proximal part of the dorsal face.

Dorsal view

The anterior part of the *facies articularis talaris posterior* is elongated anteroposteriorly. The *facies articularis talaris media* is slightly concave, and distolaterally to proximomedially oblique. The two *facies articularis* are separated by a shallow groove. The *facies articularis cuboidea* is oblique proximomedially/distolaterally. The *processus peronealis* is laterally projecting and elongated.

Plantar view

The shaft of *tuber calci* is mediolaterally compressed, and widens proximally in the *tuber calci* which is proximally convex. The *sustentaculum tali* is strongly medially projecting, forming almost a right angle with the *tuber calci*. Its lateral border is distolaterally to proximomedially oriented, parallel to the axis of the *facies articularis cuboidea*. The groove of the *sustentaculum tali* is deep. The *sulcus tendinis musculus peroneus longi* is wide and deep.

Lateral view

The lateral surface is flat, slightly concave under the *facies articularis tali posterior*. The ovoid *processus peronealis* is slightly oblique distodorsally to proximoprantarly. It is divided into two parts by a deep, narrow groove. The plantar tubercle is weak.

Medial view

Only the distal part of the medial face is visible. The plantar border is slightly concave. The *sustentaculum tali* is thin and proximodorsally/distoplantarly oblique. The groove of the *sustentaculum tali* is very weak.

Proximal view

The *tuber calci* is convex and ovoid. It is tall and oriented dorsolaterally to medioplantarly.

Distal view

The *processus peronealis* is obliquely plantarly oriented. The *facies articularis cuboidea* is taller than wide, concave and shows a notch in its medial side. The groove between the *sustentaculum tali* and the *facies articularis cuboidea* is deep.

Only the external part of the *trochlea tali* of the astragalus is preserved, articulated with the left calcaneum (Fig. 18). The upper border of the *trochlea tali* is rounded and wide. The *facies malleolaris lateralis* is not prominent, slightly concave, fused with the *processus lateralis tali*. This small processus is triangular and slightly distolaterally projecting. The *facies articularis calcanea posterior* is wide.

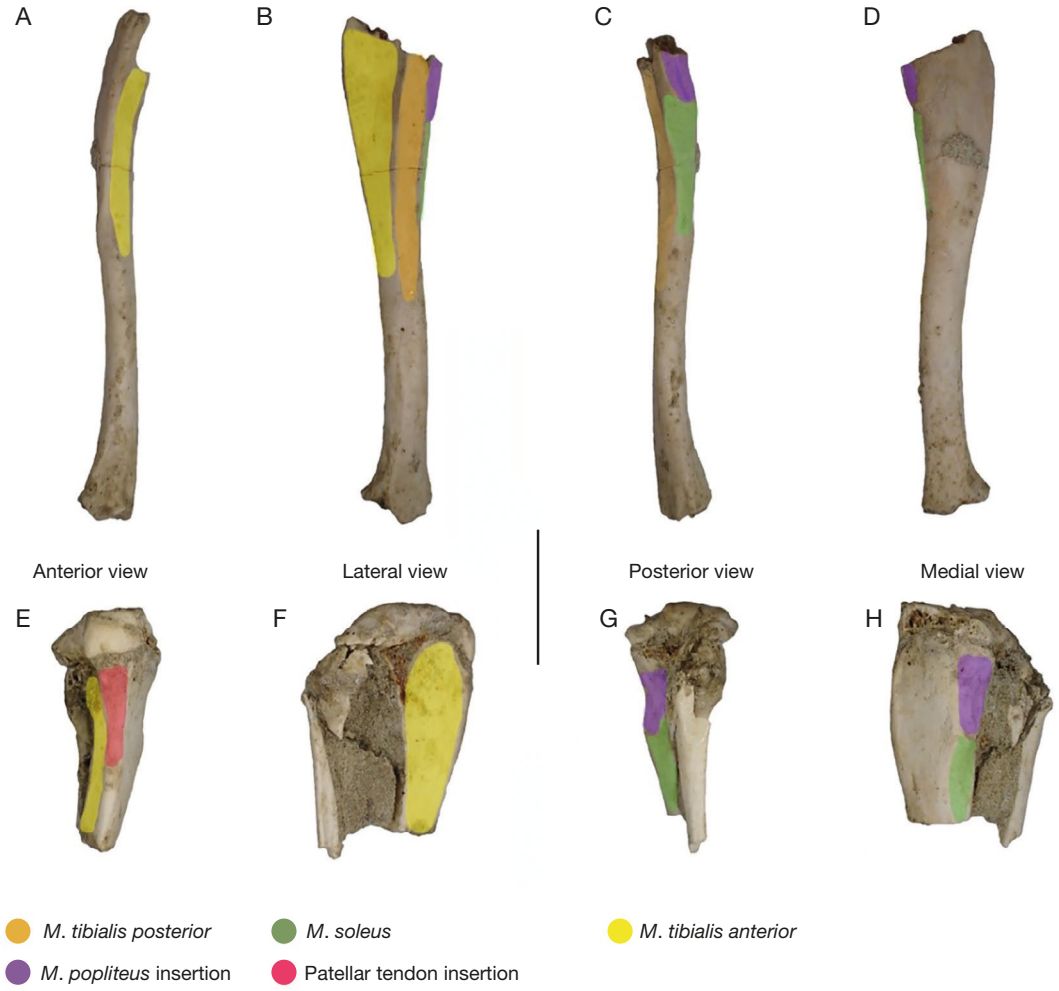

Fig. 17. — Muscular insertions on the left tibia GT 50'06. Scale bars: 1 cm.

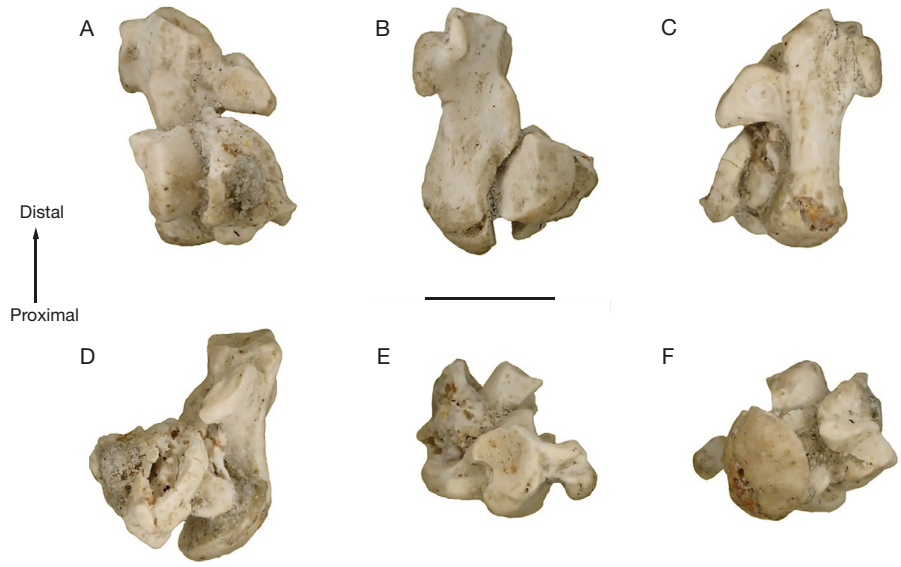

Fig. 18. — Left calcaneum of GT 50'06: **A**, dorsal view; **B**, lateral view; **C**, plantar view; **D**, medial view; **E**, distal view; **F**, Proximal view. Scale bar: 1 cm.

Fig. 19. — Rib cage GT 50'06. Scale bar: 1 cm.

Fig. 20. — Cervical vertebrae of GT 50'06: **A**, Ventral view; **B**, Dorsal view. Scale bar: 1 cm.

Fig. 21. — Lumbar vertebrae of GT 50'06 (dorsal view). Scale bar: 1 cm.

Fig. 22. — Caudal vertebrae of GT 50'06 (dorsal view).

Appendicular Skeleton (Figs 19-22)

Parts of the ribs and the vertebral column are preserved but are not complete comprising part of the rib cage, the cervical vertebrae and parts of the dorsal, lumbar and caudal vertebrae.

Part of the rib cage is preserved, partly crushed and does not permit a detailed description. The ribs seem to be thick. The cervical vertebrae are compact (but not fused as is sometimes the case in burrowing rodents) suggesting a shortened neck, the usual feature in fossorial mammals. The atlas is poorly preserved but one of the superior articular facets is preserved and deep. On the axis, the odontoid process is stout and slightly ventrally inclined.

The sacrum was not found; it is thus not possible to estimate the number of sacral vertebrae and to determine whether there was fusion with the lumbar vertebrae. The number and length of the caudal vertebrae suggests that the tail was not strongly reduced in length, unlike the case in extant subterranean mammals.

DISCUSSION

Nomenclature and dental morphology

Different authors adopt different nomenclatures to describe the structure of the cheek teeth. It can affect the interpretation of the tooth as shown by the discussion concerning the lower molars of *Bathyergoides neotertiarius*. According to the terminology of Gomes Rodrigues & Šumbera (2015), the protoconid and the metaconid are connected by a short metalophulid I, forming the anterior wall of the tooth. This crest extends anteriorly from the protoconid and to the anterolingual side of the metaconid. As such, the name "metalophulid I" for this crest agrees with the terminology of Wood & Wilson (1936).

In many rodents, the anterior wall of the cheek teeth is formed by an « anterolophid », which connects the protoconid and the metaconid. It is thus necessary to resolve the issue of homology. However, the name « metalophulid I » seems correct, according to its position (homology of position) following Wood & Wilson (1936). The fusion of the protoconid/metalophulid I/metaconid complex, due to the wear of the tooth, results in the formation of an anterior crest. It exhibits a bulge at its lingual half, which is absent in the two other crests of the molar.

According to Gomes Rodrigues & Šumbera (2015), the hypoconid is connected to the entoconid by a short crest, the entolophid. Following Wood & Wilson (1936), two crests are present between the hypoconid and the entoconid: the hypolophulid I and II. In *Bathyergoides neotertiarius*, only one crest is present, which could be named « hypolophulid » which connects the two principal cusps. This would agree with Mein & Freudenthal (1971), and would correspond to the hypolophid described by Marivaux *et al.* (2005). However, we could consider this crest to be an "entolophid", connected to the entoconid, as it would originate from the entoconid and not from the hypoconid. Only the study of the homologies between these structures and the embryological processes will permit resolution of the question, but that is not the focus of this paper.

There is a second problem concerning the metacone morphology. In the Lower Miocene species *Renefossor songhorensis*, Mein & Pickford (2008) described a short metaloph in the upper molars, connected with the lingual face of the metacone. Discovered in the Miocene Ugandan sites of Napak, this species shows a bathyergid-like dental morphology, which is very close to that of *Bathyergoides neotertiarius*. The dental morphology of the extant Bathyergidae is slightly different, showing two lophs in the upper teeth, without a short metaloph (Gomes Rodrigues & Šumbera 2015). The light wear of the M2 of GT 50'06 shows an isolated structure that could indicate the presence of an individualized cuspid (the metacone) transversely stretched. Thus, this morphology might imply the absence of a metaloph in the upper cheek teeth of *Bathyergoides neotertiarius*, close to the described morphology of the extant Bathyergids but different from the Ugandan species *Renefossor songhorensis*. However, this stretching could result from the fusion of the metacone and the short metaloph mentioned by Mein & Pickford 2008. Once again, only the study of the embryological processes will resolve the question, especially for highlighting the structures involved in this part of the M2 in extant species.

COMPARISONS WITH EXTANT FOSSORIAL RODENTS

Dental and skull/mandible morphology

Dental morphology

The dental morphology of GT 50'06 is characteristic of the extant bathyergids, allowing an assignment of the species *Bathyergoides neotertiarius* to this family. There is a difference in the presence of four lower cheek teeth (a premolar and three molars) against five mentioned by Lavocat (1973) (probably a lapsus). However, extant bathyergids such as *Bathyergus janetta*, *Cryptomys damarensis*, *Heliophobius argentocinereus* or *Georychus capensis* Pallas, 1778 have four lower cheekteeth (p4/dp4, m1, m2 and m3), corresponding to the dental formula of the Miocene species. The morphology of the dental structures of *Bathyergoides neotertiarius* is close to those of the genus *Bathyergus* and *Georychus*, showing three principal crests on the lower cheek teeth and two principal lophs on the upper teeth (Gomes Rodrigues & Sumbera 2015), depending on the different interpretations about the presence or not of the metaloph.

The incisors of GT 50'06 are extremely robust, extending beyond the m3 in the lower jaw. The fragmentary state of the skull doesn't allow determination of how far the upper incisors are implanted, however, an upper incisor fragment has been found, as robust as the lower ones. Today, many fossorial rodent species dig their burrows with their incisors (Shimmer 1903; Hildebrand 1985; Happold *et al*. 2013). This is the case with bathyergids such as *Bathyergus*, *Georychus*, *Cryptomys* and *Heliophobius*, and with the spalacid *Tachyoryctes* (Happold *et al.* 2013). Compared to the rodents with other locomotor behaviours (arboreal or terrestrial for example), the incisors of Bathyergidae are much more robust and have a deeper implantation in the skull and mandible, providing great strength during their use for burrowing (Jarvis & Sale 1971; Hildebrand 1985; Happold *et al.* 2013). Compared with the incisors of the extant species, GT 50'06 has a similar robustness and implantation, suggesting a significant use of these teeth. This morphology could indicate a burrowing mode for the Miocene species close to that of extant bathyergids and spalacids, suggesting a similar locomotor behaviour for *Bathyergoides neotertiarius*.

Skull

Despite the poor preservation of the skull, GT 50'06 is rather big (minimal width 3.82 cm), comparable to the species *Bathyergus suillus* (Table 2). As for the bathyergids *Heliophobius argentocinereus*, *Georychus capensis* and *Cryptomys hottentotus*, the enlargement of the zygomatic arch is important, reflecting the strong musculature and robusticity of the skull characteristic of this family (Fig. 23A-H, M-N). However, in lateral view, GT 50'06 has a taller zygomatic arch than

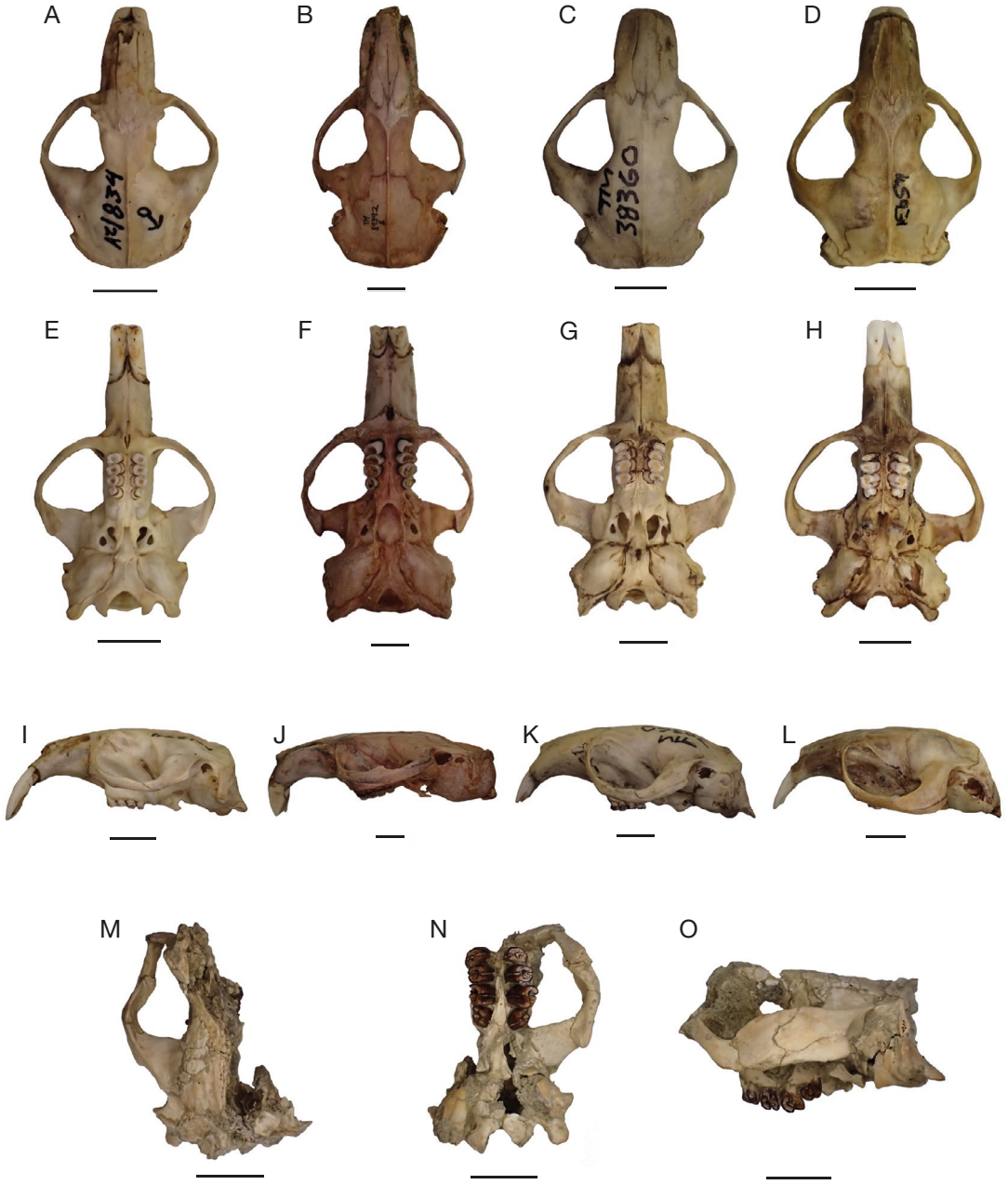

Fig. 23. — Skulls of extant fossorial rodents and GT 50'06; *Cryptomys hottentotus* AZ 834: **A**, upper view; **E**, palatal view; **I**, left lateral view; *Bathyergus suillus* (Schreber, 1782) TM 39392: **B**, upper view; **F**, palatal view; **J**, left lateral view; *Georychus capensis* (Pallas, 1778) TM 38360: **C**, upper view; **G**, palatal view; **K**, left lateral view; *Heliophobius argentocinereus* Peters, 1846 TM 45931: **D**, upper view; **H**, palatal view; **L**, left lateral view; *Bathyergoides neotertiarius* Stromer, 1923 GT 50'06: **M**, upper view; **N**, palatal view; **O**, left lateral view. Scale bars: 1 cm.

the other species, due to the expansion of the lower part of the first half of the arch well beyond the zygomatic process of the temporal bone, and to the great development of the temporal bone on the zygomatic arch. This enlarged part of the arch is rectangular in GT 50'06, while it is rounded in the extant bathyergids (Fig. 23I-L, O). This morphology could be due to an increase in robusticity of the skull in *Bathyergoides neotertiarius*, and the powerful musculature linked to the burrowing behaviour using essentially the skull/mandible complex, more so than in *Bathyergus suillus*, *C. hottentotus* and *H. argentocinereus*. The paracondylar process of GT 50'06 is as developed as the one in extant species, almost not exceeding the occipital condyles, resulting in a similar form of the rear of the skull to the species as that of *Cryptomys* (Fig. 23I-H, N). The backward-facing foramen magnum associated with a shortened neck (of which the vertebrae can be fused in some cases), and an upright supra-occipital bone are features which have been suggested as fossorial adaptations (Hildebrand 1985). Thus, this morphology associated with the global organization of the skull of *Bathyergoides* reinforces the inference of a fossorial mode using the skull/mandible/incisor complex to dig.

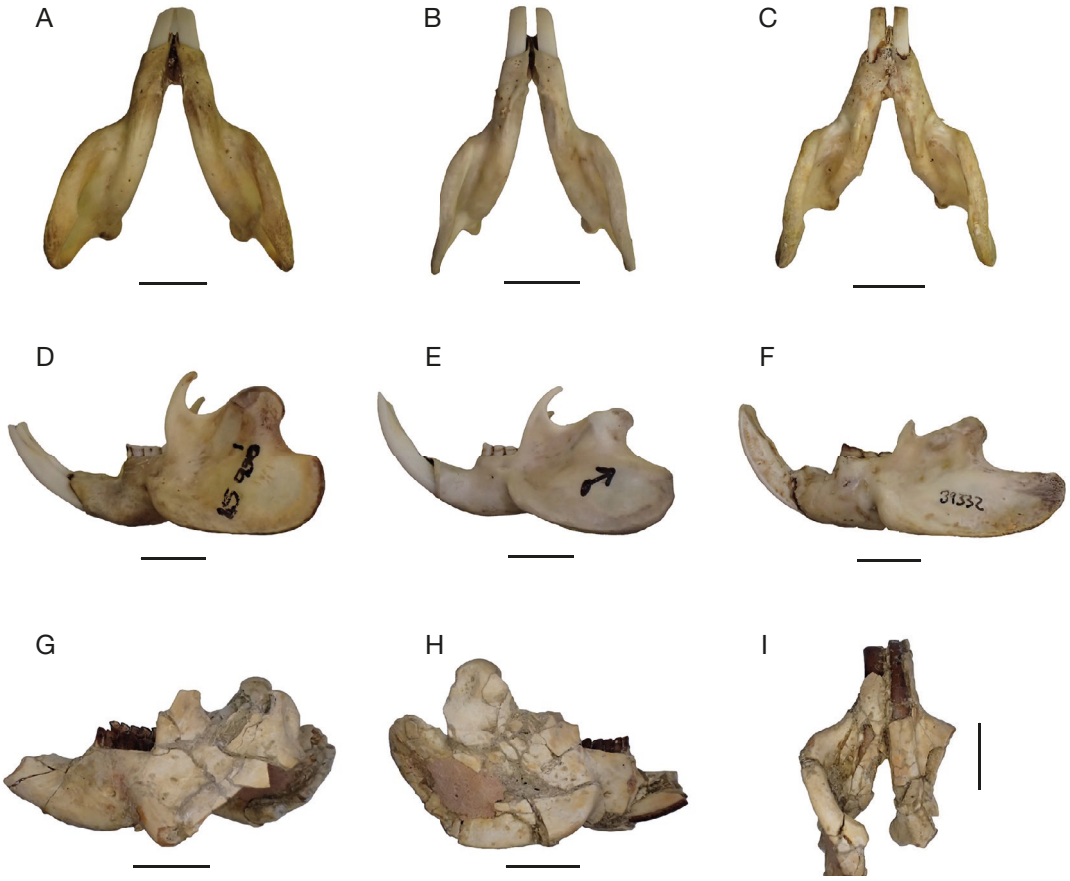

Fig. 24. — Mandible of extant fossorial rodents and GT 50'06; **A**-**C**, ventral view; **A**, *Heliophobius argentocinereus* Peters, 1846 TM 45931; **B**, *Cryptomys hottentotus* (Lesson, 1826) AZ 834; **C**; *Bathyergus janetta* Thomas & Schwann, 1904 TM 39332; **D**-**F**, left lateral view; **D**, *Heliophobius argentocinereus* Peters, 1846 TM 45931; **E**, *Cryptomys hottentotus* (Lesson, 1826) AZ 834; **F**, *Bathyergus janetta* Thomas & Schwann, 1904 TM 39332; **G**-**I**, *Bathyergoides neotertiarius* Stromer, 1923 GT 50'06; **G**, left lateral view; **H**, right lateral view; **I**, ventral view. Scale bars: 1 cm.

Table 2. — Measurements of the skull and mandible of extant fossorial rodents and *Bathyergoides neotertiarius* Stromer, 1923 (cm).

		Skull			Hemi-mandible	
Species	**Specimen numbers**	**Width**	**Length**	**Length of the cheekteeth row**	**Length**	**Length of the cheekteeth row**
C. damarensis	TM 45891	2.5	3.38	0.45	2.76	0.44
C. damarensis	TM 45578	2.39	3.31	0.47	2.48	0.51
C. damarensis	TM 38340	2.49	3.27	0.36	2.53	0.32
C. damarensis	TM 45473	2.14	3.09	0.46	2.26	0.46
C. hottentotus	AZ 834	2.61	3.42	0.43	2.76	0.42
C. hottentotus	AZ 833	2.44	3.3	0.44	2.51	0.46
C. hottentotus	96 037 M 5373	2.12	3.13	0.73	2.17	0.66
C. hottentotus	96 037 M 5374	2.12	3.23	0.72	2.47	0.72
Bathyergus janetta	TM 39332	2.75	4.42	0.67	3.36	0.75
Bathyergus janetta	TM 39306	2.46	4.06	0.62	2.86	0.66
Bathyergus suillus	TM 39404	4.16	6.54	0.89	4.9	1.04
Bathyergus suillus	TM 40548	3.61	5.83	0.82	4.29	0.93
Bathyergus suillus	TM 39393	3.99	6.7	0.94	4.9	0.97
Bathyergus suillus	TM 39392	3.52	5.84	0.79	4.27	0.94
H. argentocinereus	TM 45942	2.71	3.37	0.45	2.66	0.44
H. argentocinereus	TM 45931	2.85	3.65	0.39	2.64	0.51
H. argentocinereus	96 037 M 5694	2.88	3.71	1.05	2.58	1.07
H. argentocinereus	96 037 M 5600	2.96	3.89	1.14	3.12	1.09
G. capensis	TM 38360	3.15	4.28	0.48	3.26	0.53
G. capensis	TM 41553	3.17	4.15	0.61	3.25	0.68
Bathyergoides neotertiarius	LT 200b'98	–	–	–	> 4.59	1.28
Bathyergoides neotertiarius	GT 50'06	–	–	1.13	> 4.71	1.27

Mandible

In the lower jaw of GT 50'06, there is a lateral expansion of the ramus characteristic of extant bathyergids (Fig. 24 A-C), but its proportions are different. Indeed, the masseteric fossa is larger in the Miocene species, allowing the insertion of a large and strong masseter, enhancing the inference of the importance of the skull/mandible/incisor complex while burrowing. The coronoid process is much more developed in *Bathyergoides neotertiarius* than in the extant bathyergids, probably exceeding the articular condyle as in *H. argentocinereus* and *C. hottentotus*, but larger in all the structures (Fig. 24). This process supports the *m. temporalis* which allows jaw movements, suggesting a strong reinforcement of this part of the mandible in GT 50'06 thereby strengthening the fossorial behaviour hypothesis.

Postcranial morphology

Humerus

The humerus of GT 50'06 is close in size to that of *Bathyergus janetta*, but slightly bigger (Table 3). Morphologically, it is very similar to this extant species especially in the distal epiphysis, which shows a similar expansion of the *epicondylus medialis* (Fig. 25). However, in *Bathyergus janetta* the trochlea is mediolaterally narrowed, in contrast to GT 50'06 which is wider, resembling *H. argentocinereus* and *C. damarensis* in this feature. There is a lot of variation in the expansion of the deltoid crest in extant species, expressed as a strong projection in the medial part of the humerus, whereas in the Miocene fossil, it is represented only in a wide and extensive crest in the first two thirds of the shaft. This could be due to a lesser use of the anterior limbs in *Bathyergoides neotertiarius* while burrowing, a behaviour which is observed in extant bathyergids such as *C. hottentotus* and *C. damarensis* (Happold *et al.* 2013). However, the expansion of the deltoid crest in the two proximal thirds of the humerus reinforces the use of the upper limb in a fossorial mode, the insertion of the deltoid muscle being wide and extending over more than half of the bone in order to increase the out-force of the limb in burrowing rodents (Hildebrand 1985). The length of the deltoid insertion reflects mainly the development of the *m. deltoideus* and *m. pectoralis*, abductors of the shoulders which are important in humeral flexion. The humerus of GT 50'06 is robust, a characteristic found in fossorial and semi-fossorial rodents, as well as in many fossorial mammals. Indeed, the robusticity of the shaft permits resistance to high stresses and forces imposed by the burrowing of the substrate, without breakage of the bone (Hildebrand 1985). This characteristic is confirmed by the humeral robusticity index of the Miocene species (Price 1993; Lagaria & Youlatos 2006), which is included in the values for the fossorial rodents such as *Tachyoryctes* and *Bathyergus*, and semi-fossorial rodents such as *Cricetomys* which are great burrowers using the scratch-digging strategy (Elissamburu & De Santis 2011) (Table 4). The specimen GT 50'06 shows a marked *crista tuberculi minoris*, a structure which is slightly developed in *Tachyoryctes splendens*. This structure allows the insertion of a strong *teres major* muscle, responsible for the adduction and rotation of the humerus, and of the *m. latissimus dorsi*, retractor of the humerus (Hildebrand 1985; Candela & Picasso 2008). This could be due to the use of the upper limbs to push the soil particles to the rear of the body as well as clearing the front of the tunnel when burrowing, as is seen in *Tachyoryctes*, *Heliophobius* and even in true moles (Yalden 1966; Jarvis & Sale 1971; Hildebrand 1985). However, the humeral head is more flattened in the fossil specimen and less projecting than in the extant species, the *tuberculi majus* and *minus* are less developed (Fig. 25) suggesting that the abduction and rotatory movements are not as well developed as in the modern forms.

The specimen GT 50'06 shows an enlargement of the distal epiphysis of the humerus, especially the medial epicondyle. This structure allows the attachment of the complex of flexor, pronator and supinator muscles such as the *flexor digitorum superficialis* (flexion of the second to fifth fingers and of the wrist), the *pronator teres* muscle (pronator of the fore-arm and involved in elbow flexion), the *flexor carpi radialis* (flexion of the wrist and radial abduction), the *palmaris longus* (flexion of the hand) and the *flexor carpi ulnaris* (palmar flexion, adduction of the hand and inclination of the ulna) (Parsons 1896; Hildebrand 1985). This conformation results in reinforcement of the upper limb, providing a mechanical advantage for the burrowing by dint of an increase of the in-lever and the out-force of this limb (Hildebrand 1985; Lagaria & Youlatos 2006). This morphology is observed in fossorial rodents (Fig. 25) and semi-fossorial rodents which are scratch-diggers such as *Cricetomys gambianus* (Lagaria & Youlatos 2006). Regarding the epicondylar index of the different species sharing the fossorial and semi-fossorial habits, *Bathyergoides neotertiarius* is close to the genera *Heliophobius* and *Tachyoryctes*, as well as to *Cricetomys*, being higher than the non-fossorial species and some semi-fossorial rodents (Table 4). This could be due to similar strategies shared by the Miocene species and extant burrowers, which use their upper limbs to break and push the soil particles backwards during burrowing. This prominent medial epicondyle is concordant with the short humerus and its high humeral robusticity, which is a characteristic combination observed in fossorial rodents (Hildebrand 1985; Lagaria 2004; Lagaria & Youlatos 2006).

Ulna

The general morphology of the ulna of GT 50'06 is similar to that observed in *C. damarensis* and *C. hottentotus*, but is closer to that of *T. splendens* in the curvature of the posterior face of the bone. Although the global morphology is close to that of the Bathyergidae, the depth of the groove in the lateral face seems closer to that of *T. splendens*, where this structure is very marked (Fig. 26). During digging, *T. splendens* uses its incisors to break the soil particles and uses its anterior limbs to push the soil particles to the rear of its body and turns to push it to the surface, in contrast to the other fossorial rodents such as *H. argentocinereus* or *C. damarensis* which extract the particles with their lower limbs (Shimmer 1903; Jarvis & Sale 1971; Hildebrand 1985; Happold *et al.* 2013). This movement requires the presence of strong muscles allowing high mobility in the wrist and in the fore-arm. Indeed, the presence of a strong

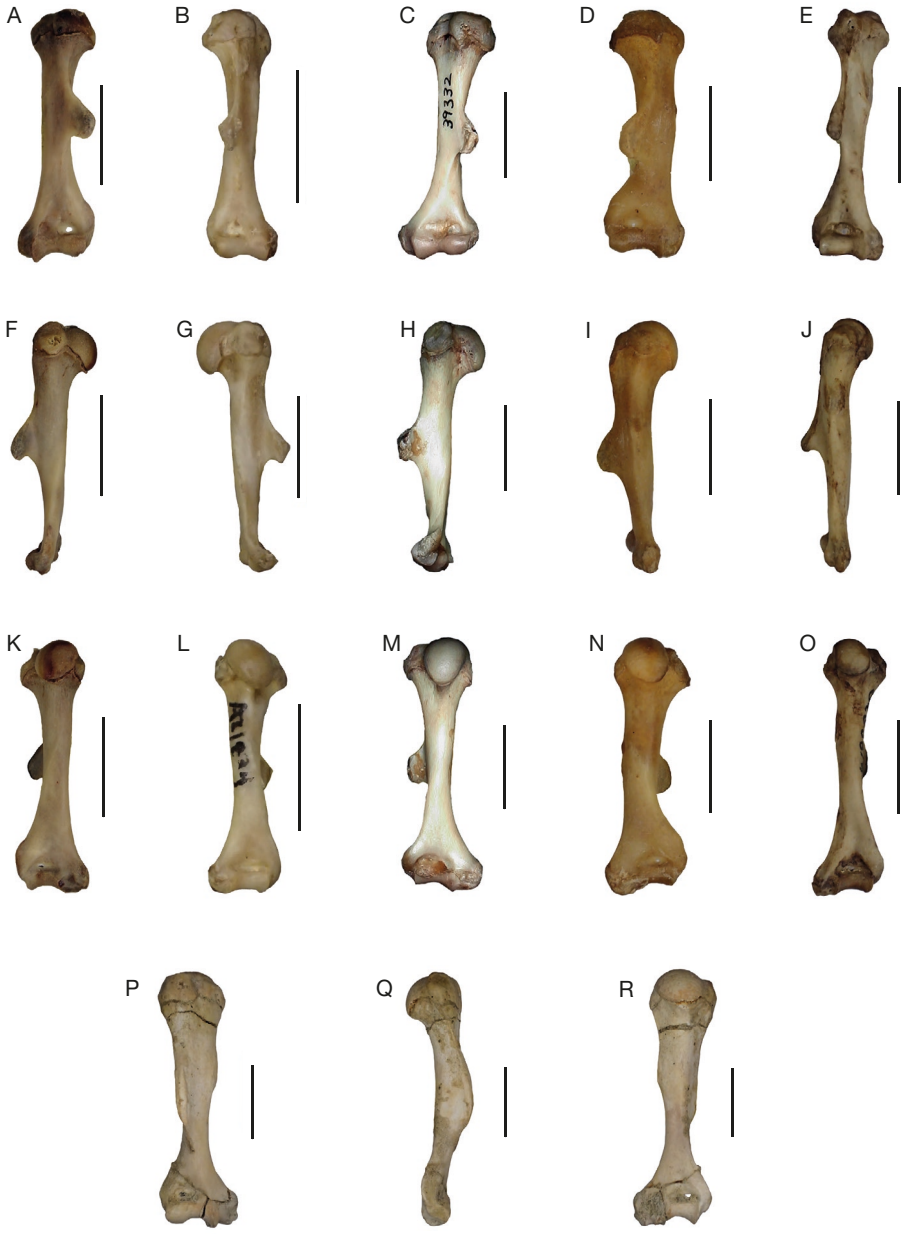

Fig. 25. — Humeri of extant fossorial rodents and of GT 50'06; *Cryptomys damarensis* (Ogilby, 1838) TM 45891, left humerus **A**, anterior view; **F**, lateral view; **K**, posterior view; *Cryptomys hottentotus* (Lesson, 1826) AZ 834, right humerus; **B**, anterior view; **G**, lateral view; **L**, posterior view; *Bathyergus janetta* Thomas & Schwann, 1904 TM 39332, left humerus; **C**, anterior view; **H**, lateral view; **M**, posterior view; *Heliophobius argentocinereus* Peters, 1846 TM 45931, right humerus; **D**, anterior view; **I**, lateral view; **N**, posterior view; *Tachyoryctes splendens* (Rüppell, 1835) 820 38 M 1, right humerus; **E**, anterior view; **J**, lateral view; **O**, posterior view; *Bathyergoides neotertiarius* Stromer, 1923 GT 50'06, right humerus; **P**, anterior view; **Q**, lateral view; **R**, posterior view. Scale bars: 1 cm.

Table 3. — Measurements of humerus of the extant fossorial rodents and *Bathyergoides neotertiarius* Stromer, 1923 (cm).

		Humerus			
Species	**Specimen numbers**	**Total length**	**Width of the shaft**	**Width of the proximal epiphysis**	**Width of the distal epiphysis**
C. damarensis	TM 45891	2.3	0.24	0.62	0.69
C. damarensis	TM 45473	2.04	0.21	0.64	0.68
C. hottentotus	AZ 834	2.38	0.26	0.73	0.68
C. hottentotus	AZ 833	2.19	0.26	0.66	0.62
Bathyergus janetta	TM 39332	2.97	0.3	0.84	0.98
H. argentocinereus	TM 45942	2.37	0.27	0.6	0.66
H. argentocinereus	TM 45931	2.46	0.37	0.74	0.82
T. splendens	820 38 M 1	2.93	0.266	0.763	0.857
T. splendens	820 38 M 2	2.68	0.236	0.733	0.845
Bathyergoides neotertiarius	GT 50'06	3.54	0.361	0.983	1.078

TABLE 4. — Osteological indices in *Bathyergoides neotertiarius* Stromer, 1923 and other fossorial/semi-fossorial and non-fossorial rodent species (Price 1993; Lagaria & Youlatos 2006*; Shepherd & Shepherd 2012; Happold et al. 2013; Bento Da Costa & Senut 2022 [this paper]).

			Index	
Group	Locomotor behaviour	n	Epicondyle (*X* ± *SD*)	Humeral robusticity (*X* ± *SD*)
Bathyergoides neotertiarius	–	–	0.305	0.102
Fossorials/semi-fossorials	–	–	–	–
Cryptomys	Fossorial	5	0.300 ± 0.018	0.111 ± 0.008
Bathyergus	Fossorial	1	0.330	0.101
Heliophobius	Fossorial	2	0.306 ± 0.027	0.132 ± 0.018
Tachyoryctes	Fossorial	2	0.304 ± 0.011	0.089 ± 0.001
Cricetomys	Semi-fossorial	3	0.299 ± 0.004	0.099 ± 0.004
*Ammospermophilus**	Semi-fossorial	10	0.242 ± 0.010	0.082 ± 0.005
*Spermophilus**	Semi-fossorial	53	0.265 ± 0.015	0.087 ± 0.008
*Cynomys**	Semi-fossorial	15	0.291 ± 0.011	0.093 ± 0.004
*Marmota**	Semi-fossorial	13	0.286 ± 0.010	0.100 ± 0.007
*Tamias**	Semi-fossorial	12	0.253 ± 0.009	0.079 ± 0.005
*Sciurotamias**	Semi-fossorial	9	0.247 ± 0.008	0.078 ± 0.004
Non-fossorial	–	–	–	–
Thryonomys	Terrestrial	7	0.260 ± 0.017	0.099 ± 0.011
Beamys	Terrestrial	1	0.254	0.086
Xerus	Terrestrial	2	0.264 ± 0.005	0.087 ± 0.001
Anomalurus	Glider	5	0.165 ± 0.007	0.065 ± 0.004
Idiurus	Glider	2	0.232 ± 0.036	0.075 ± 0.001
Petaurista	Glider	2	0.163 ± 0.003	0.061 ± 0.002
Protoxerus	Arboreal	4	0.269 ± 0.011	0.089 ± 0.005
*Protoxerus**	Arboreal	4	0.239 ± 0.003	0.083 ± 0.002
Sciurus	Arboreal	3	0.233 ± 0.021	0.078 ± 0.003
*Sciurus**	Arboreal	44	0.256 ± 0.013	0.083 ± 0.006
Ratufa	Arboreal	2	0.280 ± 0.016	0.092 ± 0.002
*Ratufa**	Arboreal	8	0.241 ± 0.015	0.082 ± 0.005
*Callosciurus**	Arboreal	12	0.252 ± 0.014	0.081 ± 0.006
*Heliosciurus**	Arboreal	3	0.224 ± 0.004	0.083 ± 0.004
*Funisciurus**	Arboreal	7	0.225 ± 0.007	0.079 ± 0.005
*Funambulus**	Arboreal	3	0.234 ± 0.006	0.077 ± 0.010
*Tamiasciurus**	Arboreal	12	0.254 ± 0.008	0.078 ± 0.004

flexor pollicis longus involved in the inclination and abduction of the wrist and in the flexion of the thumb (Parsons 1896; Hildebrand 1985) allows this type of particle extraction as seen in *T. splendens*, and could be similar to the mobility of *Bathyergoides neotertiarius* showing this deep and elongated lateral gutter on its ulnae (Fig. 26; Table 5). Furthermore, the presence of strong pronator and carpal and digital flexors which originate from the medial epicondyle of the humerus (such as the *flexor digitorum profundus*) allows an increase of the anterior limb force not only involved in the breakage of the soil particles but also in postural control during burrowing with the incisors (Hildebrand 1985; Lagaria & Youlatos 2006). So, in regard to the skull, incisors and upper limb morphologies of the Miocene species, *Bathyergoides neotertiarius* could share some similarities with the modern *T. splendens* in the use of its upper limb.

The well-developed and elongated olecranon process of GT 50'06 is similar to that of the extant fossorial rodents, close to *C. hottentotus* and *T. splendens* (Fig. 26), with a strong proximal end for the insertion of a powerful *m. triceps brachii* allowing an important pushing force linked to the elbow joint and the forearm (Hildebrand 1985; Lagaria & Youlatos 2006). The long olecranon process allows an increase of the in-lever and out-force at the level of the metacarpus, necessary for the dislocation of the soil particles during burrowing (Hildebrand 1985; Price 1993; Lagaria & Youlatos 2004). This morphology of the olecranon process is found in fossorial mammals (Shimmer 1903; Hildebrand 1985; Price 1993; Lagaria & Youlatos 2006), reinforcing the hypothesis of fossorial abilities in *Bathyergoides neotertiarius*. The sigmoid cavity is oblique, as in *C. damarensis* and *Bathyergus janetta*, suggesting outward movements of the forearm probably involved in the clearing of the burrow by extraction of soil particles and probably in the control of posture during digging.

Femur

Despite the compression of the specimen, we observe a clear difference in the thickness of the posterior limb between GT 50'06 and that of the extant fossorial species (Fig. 27). Indeed, the femur and tibia are very thin differing from the robustness seen in the extant Bathyergidae and Spalacidae. The lower limb of fossorial rodents is principally used for pushing the soil particles down from the body and in the maintenance of the posture during digging. It is less developed compared to the fore limbs, the latter showing most of the fossorial adaptations (Shimmer 1903; Hildebrand 1985; Elissamburu & De Santis 2011). However, some femoral structures are more developed in burrowing rodents such as the third trochanter and the enlargement of the muscular

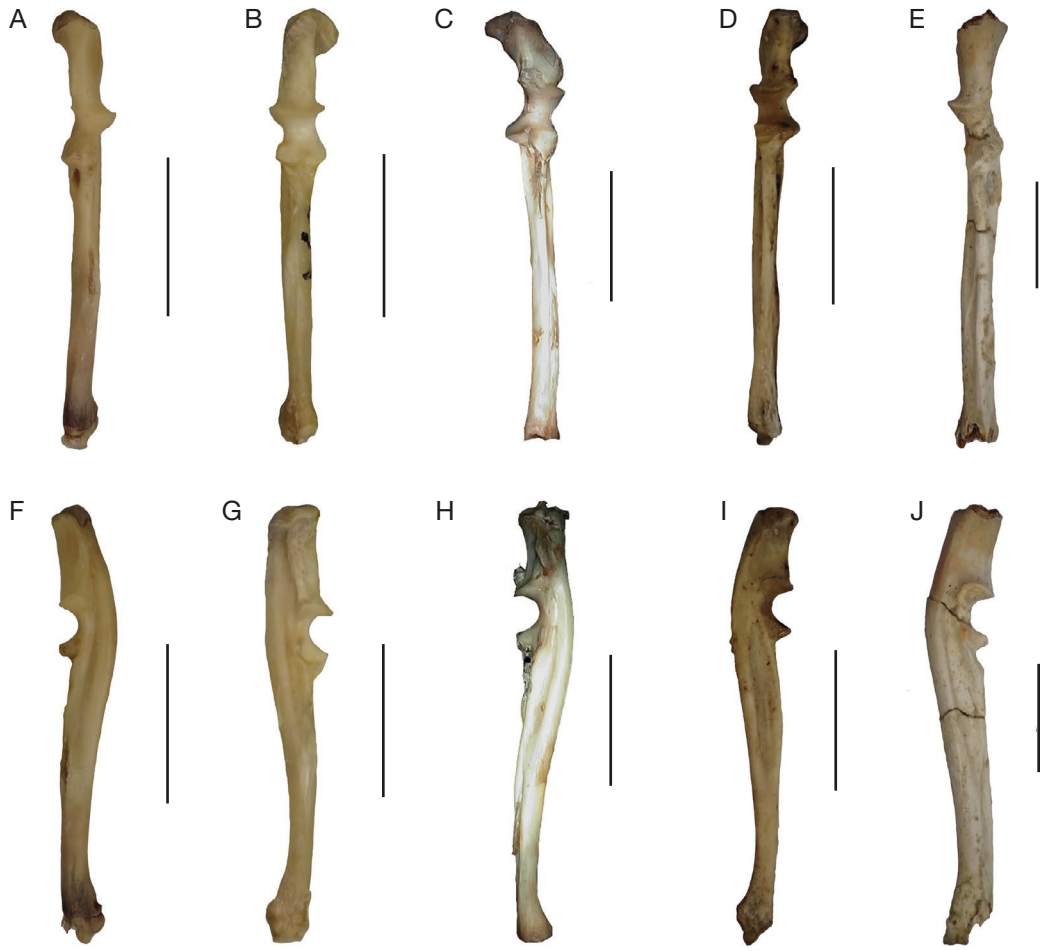

Fig. 26. — Ulnae of extant fossorial rodents and GT 50'06: *Cryptomys damarensis* (Ogilby, 1838) TM 45891, left ulna; **A**, anterior view; **F**, lateral view; *Cryptomys hottentotus* (Lesson, 1826) AZ 834, right ulna; **B**, anterior view; **G**, lateral view; *Bathyergus janetta* Thomas & Schwann, 1904 TM 39332, left ulna; **C**, anterior view; **H**, lateral view; *Tachyoryctes splendens* (Rüppell, 1835) 820 38 M 1, right ulna; **D**, anterior view; **I**, lateral view; *Bathyergoides neotertiarius* Stromer, 1923 GT 50'06, right ulna; **E**, anterior view; **J**, lateral view. Scale bars: 1 cm.

Table 5. — Measurements of the ulna of extant fossorial rodents and *Bathyergoides neotertiarius* Stromer, 1923 (cm).

		Ulna		
Species	**Specimen numbers**	**Total length**	**Width of the shaft**	**Length of the olecranon process**
C. damarensis	TM 45891	2.62	0.22	0.58
C. damarensis	TM 45473	2.24	0.17	0.47
C. hottentotus	AZ 834	2.73	0.2	0.58
C. hottentotus	AZ 833	2.61	0.19	0.55
Bathyergus janetta	TM 39332	3.34	0.26	0.53
H. argentocinereus	TM 45942	2.81	0.28	0.66
H. argentocinereus	TM 45931	2.93	0.29	0.7
T. splendens	820 38 M 1	3.587	0.217	0.596
T. splendens	820 38 M 2	3.394	0.177	0.586
Bathyergoides neotertiarius	GT 50'06	?	0.279	0.7

insertions, useful for postural control, notably in the chisel-tooth and head-lift diggers (Samuels & Van Valkenburgh 2008). Compared to the genera *Cryptomys*, *Bathyergus*, *Heliophobius* and *Tachyoryctes*, the femur of *Bathyergoides neotertiarius* shows a less-developed third trochanter, but with a marked muscular insertion surface (Fig. 27). This trochanter allows the insertion of the *gluteus maximus* muscle, responsible for the reinforcement and extension of the hips, as well as trunk straightening (Kahle *et al* 1992; Samuels & Van Valkenburgh 2008). So, the Miocene species could share a similar burrowing mode, with an involvement of the femur in postural control. In their study, O'Higgins & Milne (2013) showed the importance of the development of the third trochanter in the distribution of forces during digging by armadillos. Indeed, the forces produced by the action of the abductor muscles on the greater trochanter induce deformations in the femoral shaft, which are compen-

Fig. 27. — Femora of extant fossorial rodents and GT 50'06: *Cryptomys hottentotus* (Lesson, 1826) AZ 834, right femur; **A**, anterior view; **F**, posterior view, **K**, medial view; *Bathyergus janetta* Thomas & Schwann, 1904 TM 39332, left femur; **B**, anterior view; **G**, posterior view; **L**, medial view; *Heliophobius argentocinereus* Peters, 1846 TM 45931, left femur; **C**, anterior view; **H**, posterior view; **M**, medial view; *Tachyoryctes splendens* (Rüppell, 1835) 820 38 M 1, right femur; **D**, anterior view; **I**, posterior view; **N**, medial view; *Bathyergoides neotertiarius* Stromer, 1923 GT 50'06, left femur **E**, anterior view; **J**, posterior view; **O**, medial view. Scale bars: 1 cm.

sated by the presence of this structure. The bending strains in the femoral shaft decrease, allowing the resistance of the femur to the strong digging constraints (O'Higgins & Milne 2013). It strengthens the hypothesis of a similar use of the lower limb between extant diggers and *Bathyergoides neotertiarius*, which could have this type of force applied to its lower limb but in a lesser degree, as shown by the weaker development of its third trochanter and the thinness of the shaft.

In anterior view, the proximal epiphysis of the femur is close to that of *T. splendens*, the *tuberculus majus* not exceeding the femoral head. This extant species is a chisel-tooth digger, using the hind limbs to control its posture when burrowing, and to provide support when pushing the soil particles onto the surface with the side of the head (Jarvis & Sale 1971). These functions are assumed by the action of several muscles such as the *gluteus medius* and *minimus* which are rotators and flexors of the limb and the *piriformis* muscle which allows the rotation, abduction and retropulsion of the lower limb (Kahle *et al.* 1992). Thus, the morphology of the proximal epiphysis of *Bathyergoides neotertiarius* could reflect this digging mode, enabled by the insertion of strong rotator and abductor muscles.

In posterior view, the *tuberculus minus* is less-developed than that of the modern species, but is still marked and postero-medially projecting, as in extant diggers. This structure allows the insertion of the *iliopsoas* muscle, involved in lower limb elevation during movement, the flexion/straightening of the trunk and in the external rotation of the leg (Kahle *et al.* 1992; Samuels & Van Valkenburgh 2008). Furthermore, *Bathyergoides neotertiarius* shows a deep *fossa trochanterica*, in which the

Fig. 28. — Tibio-fibulae of extant fossorial rodents and GT 50'06: *Cryptomys hottentotus* (Lesson, 1826) AZ 834, right tibio-fibula; **A**, anterior view; **F**, postero-medial view; *Cryptomys damarensis* (Ogilby, 1838) TM 45891, left tibio-fibula; **B**, anterior view; **G**, postero-medial view; *Bathyergus janetta* Thomas & Schwann, 1904 TM 39332, left tibio-fibula; **C**, anterior view; **H**, postero-medial view; *Heliophobius argentocinereus* Peters, 1846 TM 45931, left tibio-fibula; **D**, anterior view; **I**, postero-medial view; *Tachyoryctes splendens* (Rüppell, 1835) 820 38 M 1, right tibio-fibula; **E**, anterior view; **J**, postero-medial view; *Bathyergoides neotertiarius* Stromer, 1923 GT 50'06, left tibia; **K**, anterior view; **L**, posterior view. Scale bars: 1 cm.

quadratus femoris muscle inserts, allowing the external rotation and the adduction of the thigh. Thus, the combination of those features could indicate a similar use of the hind limb in the Miocene species, although with a weaker development than in the modern burrowers, with a stabilization of the posture allowing digging with the head and mobility of the trunk.

Tibia

The tibia of *Bathyergoides neotertiarius* is very different from that of extant fossorial rodents. Beyond the compaction of the fossil specimen, we observe a strong mediolateral flattening of the bone, with a triangular tibial tuberosity extending into a thin crest until the middle of the diaphysis. Furthermore, the groove for the insertion of the *m. popliteus* is prominent, ending in its lower part by a strong protrusion. This muscle allows the flexion of the posterior limb, its internal rotation and knee stabilization (Grassé & Gabe 1967). When we join the astragalus/calcaneum complex containing the distal part of the tibia with this bone, we can see a slight inversion of the foot. Thus, a prominent *m. popliteus* could have an important role in joint stabilization and rotation of the limb during movement and the maintenance of the posture of the animal with its feet against the walls in the burrow, behaviour observed in the extant moles and mole rats such as *Tachyoryctes* and *Heliophobius* (Yalden 1966; Jarvis & Sale 1971; Hildebrand 1985). This morphology follows the same hypothesis of the importance of postural control by the hind limb during digging shown by the femoral structure.

The other difference between *Bathyergoides neotertiarius* and the extant species is the absence of fusion between the distal ends of the tibia and fibula (Fig. 28). Extant fossorial rodents show a distal fusion of these two bones, probably linked to

a reinforcement of the posterior limb (Shimmer 1903). The absence of this conformation in the Miocene species could be due to lower forces applied in those bones during digging and underground life, not requiring a really strong robustness. This assumption goes in the same direction as the thinness of the femur and tibia of GT 50'06, involving less important use during burrowing than in the modern species but showing however a real role in the digging behaviour and in particular in posture control. The left fibula shows a marked and elongated gutter, where the *flexor digitorum fibularis* muscle inserts (digital and plantar flexor), involved in "grasping" of the claws into the substrate in some rodents such as extant porcupines (McEvoy 1982; Candela & Picasso 2008). This could be in accordance with the assumption of the use of the hind limb in *Bathyergoides neotertiarius* to maintain its posture within the burrow when digging with its incisors.

Calcaneum

Unfortunately the astragalus is poorly preserved in the fossil, but the calcaneum yields a few indications concerning movements in the ankle. The body of the calcaneum (between the distal edge of the *facies articularis talaris posterior* and the *facies articularis cuboidea*) is wide and short compared to the neck, a characteristic found in fossorial taxa such as the species of *Spalax*. This feature combined with an elongated calcaneal neck is important in posture control and in pushing soil particles during digging (Carrano 1997; Ginot *et al* 2016; Davidovits 2018). The *facies articularis talaris media* and the *facies articularis cuboidea* are closer due to the shortening of the body, the latter being concave, allowing a greater mobility of the ankle (Candela & Picasso 2008). The width is mostly due to the great development of the *processus peronealis*, linked with the development of the *m. peroneus* tendons involved in the eversion and abduction of the foot. This morphology is found in extant semi-fossorial and fossorial taxa, which maintain their posture with the feet against the walls of the burrow during digging (Emry & Thorington 1982; Ginot *et al*. 2016).

In the living tree porcupines, the *facies articularis talaris posterior* is proximo-distally convex, slightly oblique, medially facing the *facies articularis talaris media* which is concave. This conformation allows a lateral movement of the astragalo-calcaneal complex. Furthermore, the two facies are separated by a deep groove. This morphology facilitates the lateral movements of this complex, linked to foot inversion, with a restraint caused by the separation of the facies (Candela & Picasso 2008). Although these extant species are arboreal, the locomotor adaptations to grasping during climbing are similar to the fossorial and semi-fossorial adaptations in living burrowers, due to the similar movements involved in climbing and in postural control during digging, and in the movements inside the burrows (Emry & Thorington 1982; Candela & Picasso 2008; Ginot *et al.* 2016). The Miocene species *Bathyergoides neotertiarius* shows a similar calcaneal organization, supporting the inference of fossorial behaviour with the hind limb involved in posture control. Finally, GT 50'06 shows an ovoid, tall and wide *tuber calci*. This structure permits the insertion of the Achilles tendons (tendons of the *m. soleus* and *m. gastrocnemius*), allowing the generation of strong forces linked to the in-lever of the foot. This morphology is generally found in fossorial and semi-fossorial taxa (*Spalax* for example) and in plantigrade species (Carrano 1997; Candela & Picasso 2008; Ginot *et al*. 2016). These observations reinforce the inference of burrowing in the Miocene species, similar to that of extant ones. However, the neck of the calcaneum seems not to be as robust as that of the extant diggers, maybe due to lesser forces applied in the hind limb during digging, as well as a possible difference in the burrow substrate, which could have been softer in the locality of Grillental during the lower Miocene.

Tail

The morphology of the subterranean animals is often linked with a short or absent tail, as observed in extant Bathyergidae or Spalacidae (Nevo 1995). Contrary to the modern fossorial subterranean species, the number and length of the caudal vertebrae in *Bathyergoides neotertiarius* suggest that it had a long tail. The length of the tail can be influenced by the ecology of the animal, using this structure for an optimal movement in their environment. Usually, a long tail is observed in arboreal rodents and gliders, important for stabilization in arboreal locomotion as well as for the increase of braking forces, balance and steering during gliding. In the burrows, a long tail can be associated with an increase of hazard, because of the capacity of predators to catch this structure during the escape of the prey (Hayssen 2008). However, some fossorial mammals possess a long tail, such as the non-subterranean scratch-digger rodent *C. gambianus* or even the armadillos and pangolins, using it for balance, support or as a gripping organ during burrowing. In some large scratch-diggers, the tail allows the increase of out-forces by maintaining the posture over the fore limbs, applying the body weight on the digging tools in order to begin burrow construction (Hildebrand 1985). It could be the case with *Bathyergoides neotertiarius*, showing this particular tail morphology, different from extant Bathyergids. Another reason for the presence of a long tail has been demonstrated by some studies, putting forward the role of this structure in thermoregulation of subterranean rodents in their burrows (Hamilton & Heppner 1967; Heppner 1970; Muchlinski & Shump 1979; Hildebrand 1985). First, among the Sciuridae, the wrapping of the tail around the body allows minimising of heat loss by increasing the thickness of the insulating layer. Thus, during exposure to cooler conditions, the body is protected and the heat keep inside, especially during feeding in cold environments (Muchlinski & Shump 1979). Secondly, the increase in insulation allows a decrease in heat assimilation in an environment where the thermal gradient promotes heat gain (Hamilton & Heppner 1967; Heppner 1970; Muchlinski & Shump 1979). This phenomenon has been observed in Sciuridae such as *Tamiasciurus hudsonicus* and *Sciurus niger*, which increase insulation by wrapping their tails around the body and decreasing heat penetration by reflecting the radiant energy of the sun by the light tail coloration (Muchlinski & Shump 1979). Finally, the tail can be used as a heat generator for cooler microen-

vironments (Hamilton & Heppner 1967; Heppner 1970; Muchlinski & Shump 1979, Hildebrand 1985). Indeed, some subterranean rodents such as gophers and desert ground squirrels store the sun's energy in their tail, radiating this energy into the burrows when the temperature decreases. This strategy is a major adaptation in arid areas, allowing resistance to heat stresses by regulating the body and microenvironmental temperature in burrows (Bartholomew & Hudson 1961; Muchlinski & Shump 1979; Hildebrand 1985). During the lower Miocene, the climate in the Namib area was more humid and warmer than it is today (Pickford *et al*. 2000; Segalen *et al*. 2002). The species *Bathyergoides neotertiarius* could have had this type of thermoregulation system, being in environments with high temperatures and/or environments with high temperature variations requiring a heating of the burrow chambers. However, the two former hypothesis could be valid for this species, the different strategies being possible in such environment.

In summary, the specimen GT 50'06 shows fossorial adaptations, close to those of extant burrowers such as the Bathyergids and Spalacids using the chisel-tooth strategy but also to the scratch-diggers. Its morphology reflects a digging strategy using principally the skull/mandible/incisor complex and the forelimb, which show an important robustness and large muscular insertions allowing the construction of burrows. The development of the distal humeral structures such as the medial epicondyle and of the ulnar structures (large olecranon process, wide lateral gutter) indicates the application of strong forces to the forearm and increase in mobility of this limb, necessary for digging. There is however a difference in the hind limbs of *Bathyergoides neotertiarius*, which are thinner, accentuated in the tibia, and an absent tibia/fibula fusion at the distal end of the bones. This type of conformation could be due to lesser use of the hind limb during movement or a softer substrate in the locality of Grillental during the lower Miocene. However, muscular insertions present on this limb such as the *m. popliteus* insertion and *m. gluteus* indicate strong stabilization and the capacity of rotational movements useful in posture control, morphologies observed in extant burrowers using chisel-tooth digging as well as the scratch digging strategies. The calcaneum provides clues that reinforce the fossorial adaptation of the Miocene species by the presence of structures allowing high joint mobility such as the expansion of the *processus peronealis* and the disposition of the *facies articularis talaris posterior* and *media*. This mobility is coupled with a reinforcement of the ankle and particularly in a strong in-lever, important in posture control. Finally, the presence of a long tail is really different from the extant chisel-tooth diggers and is closer to the morphology of the extant scratch-diggers such as members of the genus *Cricetomys*. The analysis of the precise morphology of the caudal vertebrae could be interesting to test the possible role of this structure in posture control but it is beyond the scope of this paper. All those elements allow us to assign *Bathyergoides neotertiarius* to a fossorial locomotor mode, showing adaptations to different digging strategies between chisel-tooth digging and scratch digging.

CONCLUSION

The specimen GT 50'06 allows us to improve knowledge about the Miocene species *Bathyergoides neotertiarius*. It belongs to Bathyergidae (Waterhouse, 1841), a family which is well-represented today. The fossil species is principally known by craniodental remains and the fragmentary skeleton described herein provides information about its postcranial morphology for the first time. The general morphology shows some similarities to extant rodents such as the genera *Cryptomys*, *Bathyergus* and *Heliophobius*, which are adapted to a fossorial lifestyle. The robustness of the skull/mandible/incisor complex approaches GT 50'06 closer to the genera *Cryptomys* and *Heliophobius*, which burrow essentially using the incisors, involving the reinforcement of those structures linked to the development of strong *temporalis* and *masseter* muscles. Similarly, the postcranial elements of the fossils are consistent with fossorial behaviour, close to that of the burrowing mode of *Tachyoryctes*, notably with rather robust upper limbs, an internal orientation of the ulna allowing it to push back the loose soil during digging but also a well-developed olecranon process suggesting an important leverage effect. However, there is a difference in the lower limb which is less robust than in the extant fossorial species, with an accentuated thinness of the tibia, showing an important mediolateral compression. This morphology could be due to a lesser (or different) use of this limb, privileged for posture control, notably with a developed *popliteus* muscle allowing joint stabilization of the knee. The main difference consists of the presence of a long tail, being much closer to extant scratch-diggers than to the subterranean chisel-tooth diggers. This analysis being mainly descriptive, the hypothesis about the locomotor behaviour must be tested, especially via biometric analysis and geometric morphometry, in order to discuss the inferred lifestyle of this Miocene species. From a more evolutionary aspect, the fossil from Grillental can help us to understand the evolution of the fossorial activities of the mole rats, showing fossorial adaptations close to different digging strategies.

Acknowledgements
We would like to thank the French Embassy in Namibia, the Cooperation Service of the French Embassy in Windhoek, the Collège de France, the CNRS and the Muséum national d'Histoire naturelle, Paris. Thanks to the Geological Survey of Namibia and the Ministry of Mines and Energy for providing logistic help. Thanks also to the Namibian National Monuments Council and to Namdeb Diamond Corporation (Pty) for authorisation and access to the Sperrgebiet. This work is part of a PhD project funded by Sorbonne Université, Paris, under the doctoral program "Interface Pour le Vivant". We thank Dr M. Pickford for his comments and for revision of English. We thank the reviewers Sophie Montuire and the second anonymous one for suggestions and remarks which help to improve the article.

REFERENCES

Bartholomew G. A. & Hudson J. W. 1961. — Desert ground squirrels. *Scientific American* 205 (5): 107-117. https://doi.org/10.1038/scientificamerican1161-107

Candela A. & Picasso B. 2008. — Functional anatomy of the limbs of Erethizontidae (Rodentia, Caviomorpha): indicators of locomotor behaviour in Miocene porcupines. *Journal of Morphology* 269 (5): 552-593. https://doi.org/10.1002/jmor.10606

Carrano T. 1997. — Morphological indicators of foot posture in mammals: a statistical and biomechanical analysis. *Zoological Journal of The Linnean Society* 121 (1): 77-104. https://doi.org/10.1111/j.1096-3642.1997.tb00148.x

Davidovits P. 2018. — *Physics in Biology and Medicine*. Academic Press, London, 352 p.

Elissamburu A. & De Santis L. 2011. — Forelimb proportions and fossorial adaptations in the scratch-digging rodent *Ctenomys* (Caviomorpha). *Journal of Mammalogy* 92 (3): 683-689. https://doi.org/10.1644/09-MAMM-A-113.1

Emry R. J. & Thorington R.W. 1982. — Descriptive and comparative osteology of the oldest fossil squirrel *Protosciurus* (*Rodentia: Sciuridae*). *Smithsonian Contributions to Paleobiology* 47: 21-28. https://doi.org/10.5479/si.00810266.47.1

Ginot S., Hautier L., Marivaux L. & Vianey-Liaud M. 2016. — Ecomorphological analysis of the astragalo-calcaneal complex in rodents and inferences of locomotor behaviours in extinct rodent species. *PeerJ* 4: e2393. https://doi.org/10.7717/peerj.2393

Gomes Rodrigues H. & Šumbera R. 2015. — Dental peculiarities in the silvery mole rat: an original model for studying the evolutionary and biological origins of continuous dental generation in mammals. *PeerJ* 3: 1-19. https://doi.org/10.7717/peerj.1233

Grasse P-P. & Gabe M. 1967. — *Traité de Zoologie: Anatomie, Systématique, Biologie*. Tome 16 : Mammifères, Fascicule 1. *Téguments et squelette*. Masson, Paris, 1162 p.

Hamilton W. J. & Heppner F. H. 1967. — Radiant solar energy and the function of black homeotherm pigmentation: an hypothesis. *Science* 155: 196-197. https://doi.org/10.1126/science.155.3759.196

Happold M., Kingdon J., Happold D., Butynski T., Hoffmann M. & Kalina J. 2013. — Rodentia, *in* Happold D. C. D. (eds), *Mammals of Africa*. A & C Black 3: 784 p.

Hayssen V. 2008. — Patterns of body and tail length and body mass in Sciuridae. *Journal of Mammalogy* 89 (4): 852-873. https://doi.org/10.1644/07-MAMM-A-217.1

Heppner F. 1970. — The Metabolic Significance of Differential Absorption of Radiant Energy by Black and White Birds. *The Condor* 72 (1): 50-59. https://doi.org/10.2307/1366474

Hildebrand M. 1985. — Digging in quadrupeds, *in* Hildebrand M., Bramble D. M., Liem K. F. & Wake D. B. (eds), Functional Vertebrate Morphology. *Cambridge: Harvard University Press* 89-109.

Jarvis J. U. M. & Sale J. B. 1971. — Burrowing and Burrow Patterns of East African Mole Rats *Tachyoryctes*, *Heliophobius* and *Heterocephalus*. *Journal of Zoology, London* 163: 451-479. https://doi.org/10.1111/j.1469-7998.1971.tb04544.x

Kahle W., Leonhard T. H. & Platzer W. 1992. — Anatomie 1. Appareil locomoteur. *Flammarion Médecine-Sciences*, Paris 434 p.

Lagaria A. 2004. — Morphological adaptations of the forelimb of sousliks, *Spermophilus citellus* (Rodentia, Mammalia) to scratch-digging. B.S. thesis, *University of Thessaloniki*, *Thessaloniki*, *Greece.* [In Greek.]

Lagaria A. & Youlatos D. 2006. — Anatomical correlates to scratch digging in the forelimb of European Ground Squirrels (Spermophilus citellus). *Journal of Mammalogy* 87 (3): 563-570. https://doi.org/10.1644/05-MAMM-A-251R1.1

Lavocat R. 1973. — Les rongeurs du Miocène d'Afrique Orientale : 1. Miocène inférieur. *Mémoires et Travaux de l'Institut de Montpellier* 1: 1-284.

Marivaux L., Ducrocq S., Jaeger J. J., Marandat B., Sudre J., Chaimanee Y., Tun S. T., Htoon W. & Soe A. N. 2005. — New remains of *Pondaungimys anomaluropsis* (Rodentia, Anomaluroidea) from the latest middle Eocene Pondaung Formation of Central Myanmar. *Journal of Vertebrate Palaeontology* 25 (1): 214-227. https://digitallibrary.amnh.org/handle/2246/1020

McEvoy J. S. 1982. — Comparative myology of the pectoral and pelvic appendages of the North American porcupine (*Erethizon dorsatum*) and the prehensile-tailed porcupine (*Coendou prehensilis*). *Bulletin of the American Museum of Natural History* 173 (4): 337-421.

Mein P. & Freudenthal M. 1971. — Les Cricetidae (Mammalia, Rodentia) du Néogène Moyen de Vieux-Collonges. Partie 2 : *Cricetodontidae incertae sedis*, *Melissiodontinae*, *Platacanthomyinae*, et *Anomalomyina*e. *Scripta Geologica* 60: 1-11.

Mein P. & Pickford M. 2008. — Early Miocene Rodentia from the northern Sperrgebiet, Namibia. *Memoir of the Geological Survey of Namibia* 20: 235-290.

Muchlinski A. E. & Shump K. A. 1979. — The sciurid tail: a possible thermoregulatory mechanism. *Journal of Mammalogy* 60 (3): 652-654. https://doi.org/10.2307/1380118

Nevo E. 1995. — Mammalian evolution underground. The ecological-genetic-phenetic interfaces. *Acta Theriologica* 3: 9-31. https://doi.org/10.4098/AT.arch.95-43

O'Higgins P. & Milne N. 2013. — Applying geometric morphometrics to compare changes in size and shape arising from finite elements analyses. *Hystrix, the Italian Journal of Mammalogy* 24 (1): 126-132. https://doi.org/10.4404/hystrix-24.1-6284

Parsons F. G. 1896. — Myology of rodents. Part II. An account of the myology of the Myomorpha, together with a comparison of the muscles of the various suborders of rodents. *Proceedings of the Zoological Society of London* 159-192. https://doi.org/10.1111/j.1096-3642.1896.tb03033.x

Pickford M. 2008. — Geology, stratigraphy and age of the Miocene fluvio-paludal and pedogenic deposits of the Northern Sperrgebiet, Namibia. *Memoir of the Geological Survey of Namibia* 20: 11-23.

Pickford M. & Senut B. 2000. — Geology and palaeobiology of the Namib Desert, southwestern Africa. *Memoir of the Geological Survey of Namibia* 18, 155 p.

Price M. V. 1993. — A functional–morphometric analysis of forelimbs in bipedal and quadrupedal heteromyid rodents. *Biological Journal of the Linnean Society* 50: 339-360. https://doi.org/10.1111/j.1095-8312.1993.tb00936.x

Roche D. 2012. — Apport de l'étude isotopique de l'émail dentaire des grands mammifères herbivores pour la reconstitution des environnements néogènes d'Afrique austral et orientale. *Thèse de doctorat, Université. Paris 6*, 256 p.

Samuels J. X. & Van Valkenburgh B. 2008. — Skeletal indicators of locomotor adaptations in living and extinct rodents. *Journal of Morphology* 269 (11): 1387-1411. https://doi.org/10.1002/jmor.10662

Segalen L., Renard M., Pickford M., Senut B., Cojan I., Le Callonnec L. & Rognon P. 2002. — Environmental and climatic evolution of the Namib Desert since the Middle Miocene: the contribution of carbon isotope ratios in ratite eggshells. *Comptes Rendus Geoscience* 334 (12): 917-924. https://doi.org/10.1016/S1631-0713(02)01837-0

Shepherd C. R. & Shepherd L. A. 2012. — A naturalist's Guide to the Mammals of Thailand and Southeast Asia. *Asia book, Bangkok,* 177 p.

Shimmer H. W. 1903. — Adaptations to aquatic, arboreal, fossorial and cursorial habits in mammals. III. Fossorial adaptations. *The American Naturalist* 444: 819-825. https://doi.org/10.1086/278368

Stromer E. 1923. — Bemerkungen über die ersten Landwirbeltier-Reste aus dem Tertiär Deutsch-Südwestafrikas. *Paläon-*

tologisches Zeitschrift 5: 226-228. https://doi.org/10.1007/BF03160370

STROMER E. 1926. — Reste Land-und Süsswasser-bewohnender Wirbeltiere aus den Diamantfeldern Deutsch-Südwestafrikas, *in* KAISER E. (eds), *Die Diamantenwuste Südwest-Afrikas*, Reimer, Berlin, 2: 107-153.

STUART C. & STUART M. 2015. — Stuarts' Field Guide to Mammals of Southern Africa: including Angola, Zambia & Malawi. *Random House Struik*, Cape Town, 456p.

WOOD A. E. & WILSON R. W. 1936. — A suggested nomenclature for the cusps of the cheek teeth of rodents. *Journal of Palaeontology* 388-391.

YALDEN D. W. 1966. — The anatomy of mole locomotion. *Journal of Zoology* 149 (1): 55-64. https://doi.org/10.1111/j.1469-7998.1966.tb02983.x

Submitted on 29 June 2020;
accepted on 23 September 2020;
published on 10 March 2022.

APPENDIX 1. — List of specimens used for the calculation of different indices.

Species	Specimen number
Bathyergoides neotertiarius Stromer, 1923	GT 50'06
Cryptomys damarensis Ogilby, 1838	TM 45891
Cryptomys damarensis Ogilby, 1838	TM 45473
Cryptomys hottentotus Lesson, 1826	AZ 834
Cryptomys hottentotus Lesson, 1826	AZ 833
Cryptomys mellandi Thomas, 1906	RG 16569
Bathyergus janetta Thomas & Schwann, 1904	TM 39332
Heliophobius argentocinereus Peters, 1846	TM 45942
Heliophobius argentocinereus Peters, 1846	TM 45931
Tachyoryctes splendens Rüppell, 1835	820 38 M 1
Tachyoryctes splendens Rüppell, 1835	820 38 M 2
Thryonomys swinderianus Temminck, 1827	RG 14926
Thryonomys swinderianus Temminck, 1827	RG 1926
Thryonomys swinderianus Temminck, 1827	RG 1928
Thryonomys swinderianus Temminck, 1827	RG 1927
Thryonomys swinderianus Temminck, 1827	RG 37043
Thryonomys swinderianus Temminck, 1827	AZ 1140
Thryonomys swinderianus Temminck, 1827	TM 46742
Cricetomys gambianus Waterhouse, 1840	MNHN 1946 57
Cricetomys emini Wroughton, 1910	CG 1956 578
Cricetomys emini Wroughton, 1910	CG 2001 1611
Beamys hindei Thomas, 1909	CG 2000 643
Xerus erythropus Geoffroy, 1803	AC 1973 159
Xerus erythropus Geoffroy, 1803	CG 2004 473
Anomalurus derbianus Gray, 1842	73 018 M 0137
Anomalurus jacksoni Winton, 1898b	RG 1931
Anomalurus jacksoni Winton, 1898b	RG 12720
Anomalurus Waterhouse, 1843	RG 28797
Anomalurus Waterhouse, 1843	RG 22253
Idiurus macrotis Miller, 1898	820 11 M 522
Idiurus macrotis Miller, 1898	CG 1999 463
Petaurista petaurista Pallas, 1766	CG 1982 843
Petaurista philippensis Elliot, 1839	CG 1960 3676
Protoxerus stangeri Waterhouse, 1842	CG 1965 113
Protoxerus stangeri Waterhouse, 1842	CG 1965 112
Protoxerus stangeri Waterhouse, 1842	CG 1965 119
Protoxerus stangeri Waterhouse, 1842	CG 1965 118
Sciurus carolinensis Gmelin, 1788	A 2721
Sciurus vulgaris Linnaeus, 1758	CG 1992 1997
Sciurus vulgaris Linnaeus, 1758	CG 2000 378
Ratufa affinis Raffles, 1821	CG 2000 378
Ratufa indica Erxleben, 1777	CG 1960 3677